ERD

UNCLASSIFIED

~~CONFIDENTIAL~~

Copy 22
RM E55C28

NACA RM E55C28

NACA

CASE FILE COPY

RESEARCH MEMORANDUM

PRELIMINARY FREE-JET PERFORMANCE OF XRJ43-MA-3 RAM-JET ENGINE AT MACH NUMBER OF 2.50

By Ivan D. Smith and William R. Prince

Lewis Flight Propulsion Laboratory
Cleveland, Ohio

SPECIAL RELEASE
Transmitted on ________
not to be indexed, referenced, or given further distribution without approval of NACA.

CLASSIFICATION CHANGED
To Unclassified
By authority of Class. Chg. Notice #1 Date 12/7/62

[redacted]

NATIONAL ADVISORY COMMITTEE FOR AERONAUTICS

WASHINGTON

UNCLASSIFIED

[redacted]

DECLASSIFIED

PRELIMINARY FREE-JET PERFORMANCE OF XRJ43-MA-3 RAM-JET ENGINE AT A MACH NUMBER OF 2.50

Ivan D. Smith
Aeronautical Research Scientist
Propulsion Systems

William R. Prince
Aeronautical Research Scientist
Propulsion Systems

Approved:

William A. Fleming
Aeronautical Research Scientist
Propulsion Systems

Bruce T. Lundin
Chief
Engine Research Division

maa - 3/25/55

DECLASSIFIED

3635

FOREWORD

To permit expeditious transmittal of performance data to those concerned, figures and a tabulation of "preliminary data" are presented herein. Preliminary data are test data that have not received the complete analysis and extensive cross-checking normally given a set of NACA data before release.

UNCLASSIFIED [redacted]

NATIONAL ADVISORY COMMITTEE FOR AERONAUTICS

RESEARCH MEMORANDUM

PRELIMINARY FREE-JET PERFORMANCE OF XRJ43-MA-3 RAM-JET ENGINE AT A MACH NUMBER OF 2.50

By Ivan D. Smith and William R. Prince

3635

CX-1

SUMMARY

The performance characteristics of the XRJ43-MA-3 model 20B3 ram-jet engine have been investigated in a free-jet facility as a part of the development program for the "Bomarc," ram-jet powered, interceptor-type missile.

The performance characteristics and combustor blow-out limits of the ram-jet engine are presented for a Mach number of 2.50, altitudes from 44,000 to 65,000 feet, Miami cold day and hot day inlet temperatures (790° and 873° R, respectively, at altitudes above 50,000 ft), and angles of attack between $\pm 7^\circ$.

The diffuser supercritical mass-flow ratio and the critical pressure recovery both decreased as angle of attack deviated from zero. The diffuser was unstable during subcritical operation. Areas of high and low Mach number developed at the diffuser outlet as pressure recovery was decreased to low engine thrust conditions. Angle of attack changed the positions of the diffuser-outlet Mach number contours, but had little effect on their severity.

A discontinuity occurred in all the performance data when combustion screech was encountered. Combustion screech, which was generally encountered in the medium-to-high fuel-air-ratio range, improved the performance, but the severity or destructiveness could not be determined because of the heavy duty engine used in this investigation. A hysteresis occurred when the fuel-air ratio was increased and decreased, taking the combustor into and out of screech.

Angle of attack and inlet temperature had little effect on engine performance, while increasing the altitude from 44,000 to 65,000 feet decreased the net thrust coefficient between 0.05 and 0.10. During combustor screech, altitude had a very small effect on engine performance.

In general, the combustor blow-out limits were decreased as altitude was increased or inlet temperature decreased.

UNCLASSIFIED [redacted]

INTRODUCTION

The performance characteristics of the XRJ43-MA-3 model 20B3 ram-jet engine have been investigated by free-jet technique in an altitude test chamber at the NACA Lewis laboratory. This investigation was conducted in cooperation with the Air Research and Development Command, U. S. Air Force, as a part of the development program for the "Bomarc," ram-jet powered, interceptor-type missile.

The interim Bomarc missile, for which this investigation was specifically conducted, requires engine operation between Mach numbers of 2.2 and 2.7 at altitudes from 30,000 to 65,000 feet. Rated thrust must be attainable at angles of attack between $\pm 4^{\circ}$ with inlet temperatures between those prescribed by the Miami cold day and Miami hot day schedules. Stable combustion must be possible at angles of attack to $\pm 7^{\circ}$ with a Miami cold day inlet temperature.

3635

The performance data presented herein include the inlet-air-flow calibration, supersonic diffuser performance, combustor performance, combustor blow-out limits, and engine net thrust coefficient at a Mach number of 2.50, altitudes from 44,000 to 65,000 feet, Miami cold day and hot day inlet temperatures (790° and 873° R, respectively, at altitudes above 50,000 ft), and angles of attack between $\pm 7^{\circ}$. Facility air-flow limits prevented operation below an altitude of 44,000 feet. Combustion data are given over a range of fuel-air ratios with three different fuel-injection methods.

APPARATUS

Facility

The installation of the XRJ43-MA-3 ram-jet engine in the altitude test chamber is shown in figure 1. Air with moisture content of approximately 9 grains per pound of air was supplied to the entrance of the supersonic free-jet nozzle at the required total pressure and temperature, and accelerated through the supersonic nozzle to the desired Mach number at the nozzle exit. The engine inlet was immersed in the supersonic stream at the nozzle exit. Angle irons and wire screens in the plenum chamber and on the supersonic nozzle inlet straightened the inlet-air profile. A jet diffuser was installed on the supersonic nozzle exit for part of this investigation, allowing a decrease in the facility pressure ratio and an increase in altitude. The supersonic nozzle was pivoted about a horizontal axis to simulate angles of attack between $\pm 7^{\circ}$. A shadowgraph system was used to determine the inlet shock pattern. The combustor in operation was observed by means of a periscope that was located downstream of the engine and that afforded a view of the combustion region through the exhaust nozzle.

3635

CX-1 back

Engine

A cross-sectional view of the heavy duty XRJ43-MA-3 ram-jet engine used in this investigation is shown in figure 2. Indicated in the figure are the diffuser inner body and longeron supports, the diffuser grid, the fuel system, the flame holder, and the instrumentation stations. The internal geometry of the heavy duty engine used is identical with the flight engine.

The projected area of the cowl lip was 0.403 and the throat area of the exhaust nozzle was 0.703 percent of the maximum combustion-chamber flow area. The inner body was supported by three equally spaced longerrons. About 1 percent of the inlet air flow was bled overboard from an air scoop in the main longeron to simulate air used by an air turbine-driven fuel pump in the flight engine. To simulate the flight installation, the engine was mounted in the altitude test chamber so that the main longeron was 45° counterclockwise at the top centerline when looking downstream. A grid, which was composed of two-dimensional airfoils (figs. 2 and 3) and had a blockage of about 38 percent, was located in the inlet diffuser. The purpose of this grid was to act as a flow-straightening screen and to optimize the position of the diffuser shock wave in order to eliminate shock-induced separation.

The engine fuel-injection system had two branches (figs. 2 and 3). One branch had 12 spray nozzles in the inner ring and 4 pairs of nozzles mounted at a radius outside the outer ring. The other branch had 16 spray nozzles in the outer ring. All spray nozzles used were a spring-loaded variable-area type. The fuel used during this investigation was clear gasoline having a hydrogen-carbon ratio of 0.182 and a lower heating value of 18,800 Btu per pound.

The flame holder used was a baffle-type with one annular V-gutter connected to the inner body by eight radial V-gutters (fig. 4). Flame-holder projected blockage of the annular area was approximately 52 percent. A propane-air system with an electric spark was located inside the section of the inner body shown in figure 4(b) and used for ignition.

Instrumentation

Instrumentation stations are shown in figures 1 and 2. Total pressures were measured at stations 0, 2, and 5; wall static pressures were measured throughout the entire length of the engine (fig. 2); and temperature was measured at station 0. All pressures were measured by mercury manometers, the wells of which were open to atmospheric pressure. Atmospheric pressure was measured by an absolute mercury manometer. All manometer readings were recorded photographically. Temperatures were recorded by a self-balancing potentiometer.

The fuel flow to each of the two branches of the fuel system was measured by a positive-displacement electronic flowmeter. These flowmeters were calibrated by comparison with standard rotameters.

Air-Flow Calibrator

The air flow through the engine is determined from the effective capture area of the supersonic diffuser and the total pressure and temperature upstream of the supersonic nozzle. (The symbols used and the 3635
calculations are presented in appendixes A and B, respectively.) Cold-flow tests with an air-flow calibrator (fig. 5) were used to determine the effective capture area of the diffuser. The diffuser total-pressure ratio was varied by means of a butterfly valve. The flow was smoothed downstream of the valve by six 2-mesh 0.062-inch wire screens so that the pressure profile and, hence, the exhaust-nozzle discharge coefficient would be the same as with combustion. The same exhaust nozzle was used on the air-flow calibrator as on the combustor.

PROCEDURE

The XRJ43-MA-3 fuel control calls for three different types of operation during flight. For low thrust, the fuel system with 20 spray nozzles (see APPARATUS) is used alone. This use is referred to as inner-ring-only operation and is used to an over-all fuel-air ratio of about 0.035. For intermediate thrusts, the inner ring is held at a fuel-air ratio of approximately 0.035 and additional fuel is injected through the system with 16 spray nozzles (outer ring) until the desired thrust is attained. This type of operation is referred to as dual-pressure and is used until the pressure in the two fuel systems is equal (approximate over-all fuel-air ratio of 0.065). For high thrust, a common fuel pressure is supplied to both fuel branches. This procedure is referred to as single-pressure operation and is used for all fuel-air ratios above 0.065. The two branches of the fuel system were controlled independently during these tests, but the types of operation encountered during flight were simulated. These types of operation were not directed specifically to the interim engine.

Data were taken at the following angles of attack with each method of fuel injection at the seven inlet conditions listed:

[redacted]

3635

Inlet temperature, T_0, $^{\circ}R$		Altitude, ft	Angle of attack, α, deg		
			Inner ring only	Dual pressure	Single pressure
Miami cold day	812	45,000	+4	+4	0,+4
	790	50,000	0,±4	+4	0,±4,-7
	790	60,000	0,±4	0,±4	0,±4
	790	65,000	0,+4	0,+4	0,+4
Miami hot day	914	45,000	+4	+4	-----
	873	60,000	±4	±4	0,±4
	873	65,000	+4	+4	+4

Data were taken over apporixmately the following fuel-air-ratio range with each fuel injection method: inner-ring-only, 0.030 to 0.050; dual-pressure, 0.040 to 0.070; single-pressure, 0.040 to 0.080. Lean blow-out data were taken with inner-ring-only fuel injection and rich blow-out data were taken with both dual-pressure and single-pressure fuel injection. To check the effect on performance of variations in the fuel control, dual-pressure fuel injection was run with the two nominal inner-ring fuel-air-ratio settings of 0.033 and 0.037.

Data were taken with and without the jet diffuser attached to the supersonic nozzle.

The combustor was ignited before the flow was established in the supersonic nozzle (i.e. with subsonic flow at the engine inlet) and then the exhaust pressure was lowered until the supersonic flow was established.

RESULTS

The engine performance data obtained are summarized in table I. Shown in graphic form are the engine-inlet air-flow calibration, diffuser-outlet Mach number contours, engine performance, and combustor blow-out limits.

The engine-inlet air-flow calibration is presented in figure 6, which gives the relation between diffuser total-pressure recovery and inlet mass-flow (or capture-area) ratio for several angles of attack at inlet temperatures of 790° (MCD) and 873° R (MHD) and an altitude of 60,000 feet. Over the range of angles of attack investigated, the supercritical mass-flow ratio decreased a maximum of 0.025 from the value at zero angle of attack. The supercritical mass-flow ratio also decreased about 0.013 as the inlet temperature was decreased from 873° to 790° R. The diffuser critical total-pressure recovery decreased about 0.03 at

$\pm 4^{\circ}$ angles of attack and about 0.06 at $\pm 7^{\circ}$ angles of attack from the value at zero angle of attack (approximately 0.66). The diffuser critical pressure recovery also decreased about 0.005 as the inlet temperature was decreased from 873° to 790° R. During subcritical diffuser operation, the inlet shock pattern interferred with the supersonic nozzle flow and changed the Mach number slightly. However, shadowgraph observations and high-speed instrumentation both indicate that the diffuser was unstable during subcritical operation.

The diffuser-outlet (station 2) Mach number contours are presented 3635
in figure 7. High combustor total-pressure loss and upstream burning will result if the Mach number variation entering the combustor is too severe. The Mach numbers were calculated from the total-pressure readings and the static pressure assuming uniform static pressure across the passage as determined from the wall static measurements at each rake. The four wall static pressures were generally within ± 0.01 of the average. Altitude, inlet temperature, and combustion had little or no effect on the diffuser-outlet Mach number contours. The effect of diffuser total-pressure recovery on the diffuser-outlet Mach number contours at zero angle of attack can be seen in figure 7(a). The difference between maximum and minimum Mach numbers increased from 0.16 to 0.49 as diffuser total-pressure recovery decreased from 0.658 to 0.421 at zero angle of attack. Variation of the diffuser-outlet contours with angle of attack is shown in figures 7(b) and (c) for diffuser total-pressure recoveries of approximately 0.595 and 0.475, respectively. Angle of attack changed the positions of the diffuser-outlet contours, but had little effect on their severity. The occurrence of combustion screech caused a shift in the diffuser-outlet contours but no increase in severity of the profile.

The performance of the engine is presented in figures 8 to 12. All performance figures show combustor-outlet total pressure, combustor total-pressure ratio, diffuser total-pressure recovery, combustor-inlet Mach number, combustion efficiency, and engine net-thrust coefficient as functions of fuel-air ratio. In this preliminary report no attempt will be made to explain trends and only a few major points will be discussed.

A discontinuity occurred in all the performance data when combustion screech was encountered. Combustion screech was generally encountered in the medium-to-high fuel-air-ratio range, and the frequency of oscillation was determined to be from 600 to 700 cycles per second. Combustion screech improved the performance, but the severity or destructiveness could not be determined because of the heavy duty (water-cooled boiler plate) engine used in this investigation. Therefore, the effect on a flight weight engine is unknown. A hysteresis occurred when the fuel-air ratio was increased and decreased, taking the combustor into and out of screech.

The engine performance at an altitude of 60,000 feet and an inlet temperature of 790° R (MCD) is shown on figure 8. Performance with the three different types of fuel injection are shown in parts (a), (b), and (c) of this figure. Angle of attack had a small effect on performance over the range investigated (between ±4°). Data at two different inner-ring fuel-air-ratio settings (0.033 and 0.037) were obtained during dual-pressure fuel-injection operation and each are indicated on part (b). This variation had a negligible effect on performance and is not indicated on all remaining performance figures. The effect of the addition of the jet diffuser to the supersonic nozzle is also shown in figure 8. The jet diffuser had a negligible effect on performance of the engine so that on succeeding figures no differentiation is made between operation with or without the jet diffuser.

3635

The engine performance at two other inlet conditions (altitude, 60,000 ft and inlet temperature, 873° R; altitude, 50,000 ft and inlet temperature, 790° R) is presented in figures 9 and 10. All three fuel-injection methods are presented on the same figure so that a direct comparison can be made between them. Inner-ring-only operation gave better performance to a fuel-air ratio of about 0.05 than dual-pressure operation. Dual-pressure and single-pressure operation gave similar results over the range of fuel-air ratios investigated. Angle of attack also had a small effect on performance at these inlet conditions.

The effect of inlet temperature on engine performance is shown in figure 11 at an altitude of 60,000 feet and an angle of attack of +4°. A slightly higher net thrust coefficient was obtained at an inlet temperature of 790° R than at 873° R.

The effect of altitude on engine performance is presented in figure 12 at the Miami cold day inlet temperatures and an angle of attack of +4°. The three fuel-injection methods are separated because of the volume of data and are shown on parts (a), (b), and (c). The net thrust coefficient decreased as altitude was increased and was between 0.05 and 0.10 lower at 65,000 feet than at 45,000 feet if the combustor was not screeching. During combustor screech, altitude had a very small effect on engine performance.

The combustor blow-out limits are presented in figures 13 and 14 for all conditions investigated. The combustor fuel-air ratio at blow-out is shown in figure 13 and the approximate diffuser total-pressure recovery at blow-out is shown in figure 14. Rich blow-out data were taken with either dual-pressure or single-pressure fuel injection (as indicated) and lean blow-out data were taken with inner-ring-only fuel injection. In general, the combustor blow-out limits were decreased as altitude was increased or inlet temperature decreased.

SUMMARY OF RESULTS

The performance of the XRJ43-MA-3 ram-jet engine, tested in a free-jet facility at a Mach number of 2.50, was as follows:

The inlet supercritical mass-flow ratio decreased a maximum of 0.025 as the angle of attack deviated from zero to $\pm 7^{\circ}$. The diffuser critical total-pressure recovery decreased about 0.03 and 0.06 at angles of attack of $\pm 4^{\circ}$ and $\pm 7^{\circ}$, respectively, from the value at zero angle of attack. The diffuser was unstable during subcritical operation. 3635

Altitude, inlet temperature, and combustion had little or no effect on the diffuser-outlet Mach number contours. The difference between maximum and minimum Mach numbers increased from 0.16 to 0.49 as diffuser total-pressure recovery decreased from 0.658 to 0.421 at zero angle of attack. Angle of attack changed the positions of the diffuser-outlet contours, but had little effect on their severity. Combustion screech caused a shift in the diffuser-outlet contours but no change in the severity of the profile.

A discontinuity occurred in all the performance data when combustion screech was encountered. Combustion screech, which was generally encountered in the medium-to-high fuel-air-ratio range, improved the performance, but the severity or destructiveness could not be determined because of the heavy duty engine used in this investigation. A hysteresis occurred when the fuel-air ratio was increased and decreased, taking the combustor into and out of screech.

Angle of attack, inlet temperature, and the two inner-ring fuel-air-ratio settings on dual-pressure fuel injection all had a small effect on performance over the ranges investigated. The net thrust coefficient decreased as altitude was increased and was between 0.05 and 0.10 lower at 65,000 feet than at 45,000 feet if the combustor was not screeching. During combustor screech, altitude had a very small effect on engine performance.

In general, the combustor blow-out limits were decreased as altitude was increased or inlet temperature decreased.

Lewis Flight Propulsion Laboratory
National Advisory Committee for Aeronautics
Cleveland, Ohio, March 25, 1955

3635

CX-2

APPENDIX A

SYMBOLS

The following symbols are used in this report:

A	area, sq ft
C	coefficient
F	thrust, lb
g	acceleration due to gravity, 32.174 ft/sec^2
M	Mach number
MCD	Miami cold day temperatures
MHD	Miami hot day temperatures
P	total pressure, lb/sq ft abs
p	static pressure, lb/sq ft abs
R	gas constant, 53.34 ft-lb/(lb)($^{\circ}$R)
T	total temperature, $^{\circ}$R
V	velocity, ft/sec
W	flow rate, lb/sec
α	angle of attack, deg
γ	ratio of specific heats
η	efficiency
ρ	density, lb/cu ft

Subscripts:

a	air
b	combustor

d	discharge
f	fuel
g	gas
N	nozzle
n	net 3635
0	stream tube (at free-stream conditions) having same area as engine inlet
1	engine inlet
2	diffuser outlet or combustor inlet
3	combustion chamber (28 in. diam.)
5	exhaust-nozzle throat
6	exhaust-nozzle exit

3635

APPENDIX B

METHODS OF CALCULATIONS

Combustor air flow. - The combustor air flow was determined from nonburning conditions as follows:

$$W_{a,5} = \frac{P_5}{\sqrt{T_5}} A_5 C_{d,5} \sqrt{\frac{\gamma_5 g}{R}} \left(\frac{2}{\gamma_5 + 1}\right)^{\frac{\gamma_5+1}{2(\gamma_5-1)}}$$

where A_5 is 2.996 square feet, no total-temperature loss $(T_0 = T_5)$ is assumed, and $\gamma_5 = 1.4$. Information supplied by the manufacturer and small-scale nozzle tests indicate the exhaust-nozzle discharge coefficient $C_{d,5}$ to be about 0.975. Therefore the air-flow equation is:

$$W_{a,5} = 1.553 \left(\frac{P_5}{P_0}\right) \frac{P_0}{\sqrt{T_0}} \tag{B1}$$

Very little combustion data were taken with the diffuser operating subcritically. Therefore, the diffuser supercritical air flow was used for all combustion data and P_5/P_0 = constant (for a given angle of attack and inlet temperature).

The average supercritical values of P_5/P_0 as determined from the air-flow calibration are:

Angle of attack, α, deg	Inlet temperature, T_0, $^{\circ}R$	P_5/P_0
0	790	0.2107
-4		.2087
+4		.2105
-7		.2052
+7		.2070
0	873	.2137
-4		.2114
+4		.2135
-7		.2082
+7		.2100

An inlet-air-flow calibration was not obtained at 0°, +4°, and +7° angles of attack at an inlet temperature of 873° R. Therefore, the effect of angle of attack on P_5/P_0 as determined at an inlet temperature of 790° R was also applied to the data at an inlet temperature of 873° R.

Inlet mass-flow ratio (or capture-area ratio). - A small amount of air was bled overboard to simulate that used by the air-turbine-driven fuel pump in flight. This air bleed was determined to be about 0.01 so that

$$\frac{W_{a,5}}{W_{a,1}} = 0.99$$

but 3635

$$\frac{W_{a,5}}{W_{a,1}} = \frac{1.553 \dfrac{P_5}{\sqrt{T_0}}}{\left(\dfrac{W_{a,1}}{W_{a,0}}\right) A_0 P_0 M_0 \sqrt{\dfrac{\gamma_0 g}{R T_0}} \left[1 + \dfrac{\gamma_0 - 1}{2} M_0^{\,2}\right]^{-\frac{\gamma_0 + 1}{2(\gamma_0 - 1)}}}$$

where $A_0 = A_1 = 1.7194$ square feet, $\gamma_0 = 1.4$, and

$$\frac{W_{a,1}}{W_{a,0}} = 4.524 \frac{P_5}{P_0} \tag{B2}$$

The values of P_5/P_0 were determined from the air-flow calibration.

Exhaust-gas temperature. - The exhaust-gas temperature was calculated from the following equation:

$$T_5 = \left[\frac{P_5 A_5 C_{d,5} g}{W_{g,5}} \sqrt{\frac{\gamma_5}{gR}} \left(\frac{2}{\gamma_5 + 1}\right)^{\frac{\gamma_5 + 1}{2(\gamma_5 - 1)}}\right]^2$$

where $A_5 = 2.996$ square feet, and $C_{d,5} = 0.975$.

$$f(\gamma_{5,R}) = \sqrt{\frac{\gamma_5}{gR}} \left(\frac{2}{\gamma_5 + 1}\right)^{\frac{\gamma_5 + 1}{2(\gamma_5 - 1)}}$$

Therefore,

$$T_5 = \left[\frac{94.0\, P_5\, f(\gamma_{5,R})}{W_f + W_{a,5}}\right]^2 \tag{B3}$$

$f(\gamma_{5,R})$ was determined from reference 1 and the engine fuel-air ratio.

[redacted]

Combustion efficiency. - The combustion efficiency was defined as

$$\eta_b = \frac{T_5 - T_0}{\Delta T_{ideal}} \tag{B4}$$

where ΔT_{ideal} was obtained from reference 2 using T_0 and the engine fuel-air ratio.

3635

Net thrust coefficient. - The net thrust is defined as

$$F_n = \eta_N \frac{W_{g,6}}{g} V_6 + (\eta_N p_6 - p_0)A_6 - \frac{W_{a,1}}{g} V_0$$

$$= \eta_N p_6 A_6 \left(1 + \gamma_6 M_6^{\,2}\right) - \gamma_0 p_0 \frac{W_{a,1}}{W_{a,0}} A_0 M_0^{\,2} - p_0 A_6$$

The net thrust coefficient is defined as

$$C_{F_n} = \frac{F_n}{\frac{\rho_0}{2g} V_0^{\,2} A_3}$$

but

$$\frac{\rho_0 V_0^{\,2}}{2g} = \frac{\gamma_0 p_0 M_0^{\,2}}{2}$$

and

$$C_{F_n} = \frac{\eta_N p_6 A_6 \left(1 + \gamma_6 M_6^{\,2}\right) - \gamma_0 p_0 \frac{W_{a,1}}{W_{a,0}} A_0 M_0^{\,2} - p_0 A_6}{\frac{\gamma_0}{2} p_0 M_0^{\,2} A_3}$$

where $A_3 = A_6$ and it is assumed that $P_6 = P_5$

$$C_{F_n} = \left[\frac{2\eta_N}{\gamma_0 M_0^{\,2}} \left(\frac{p_6}{P_6}\right)\left(\frac{P_0}{p_0}\right)\left(1 + \gamma_6 M_6^{\,2}\right)\right] \frac{P_5}{P_0} - 2\left(\frac{A_0}{A_6}\right)\left(\frac{W_{a,1}}{W_{a,0}}\right) - \frac{2}{\gamma_0 M_0^{\,2}}$$

where $A_0 = A_1 = 1.7194$ square feet, $A_5 = 2.996$ square feet, $A_6 = 4.276$ square feet, and it is assumed that $M_0 = 2.50$, $\gamma_0 = 7/5$, $\gamma_6 = 9/7$, $C_{d,5} = 0.975$, and $\eta_N = 0.97$. Then

$$C_{F_n} = 3.587 \frac{P_5}{P_0} - 0.8042 \frac{W_{a,1}}{W_{a,0}} - 0.2286$$

where $W_{a,1}/W_{a,0}$ was assumed to a constant for each inlet temperature and angle of attack. Values can be calculated from the table of values of P_5/P_0 (p. 11) and equation (B2).

REFERENCES 3635

1. Whitaker, R. C.: Methods for Reducing and Processing Data from Free-Jet Tests of Ramjet Engines. Rep. 5362, Marquardt Aircraft Co., Nov. 23, 1953. (Contract AF33(038)-19589, Proj. 50, Boeing P.O. 350141-952.)

2. Mulready, Richard C.: The Ideal Temperature Rise Due to the Constant Pressure Combustion of Hydrocarbon Fuels. Meteor Rep. UAC-9, Res. Dept., United Aircraft Corp., July 1947. (Proj. Meteor, Bur. Ord. Contract NOrd 9845 with M.I.T.)

TABLE I. - PRELIMINARY FREE-JET PERFORMANCE OF XRJ43-MA-3 RAM-JET ENGINE AT A MACH NUMBER OF 2.50

(a) Single-pressure fuel injection

Altitude, ft	Angle of attack, α, deg	Free-stream total temperature, T_0, °R	Free-stream total pressure, P_0, lb/sq ft abs	Combustor supercritical air flow, $W_{a,5}$, lb/sec	Diffuser outlet Mach number, M_2	Diffuser outlet total pressure, P_2, lb/sq ft abs	Exhaust nozzle total pressure, P_5, lb/sq ft abs	Diffuser total pressure recovery, $\frac{P_2}{P_0}$	Engine total pressure ratio, $\frac{P_5}{P_0}$	Combustor total pressure ratio, $\frac{P_5}{P_2}$	Fuel flow, W_f, lb/sec	Fuel air ratio, $\frac{W_f}{W_{a,5}}$	Exhaust gas total temperature, T_5, °R	Combustion efficiency, η_b	Net thrust coefficient, C_{F_n}
44,000	0	808	5551	63.89	0.318	3175	2691	0.572	0.485	0.848	3.23	0.0506	3605	0.941	0.744
		810	5503	63.27	.311	3189	2704	.580	.491	.848	3.53	.0558	3660	.904	.768
		808	5510	63.41	.294	3280	2787	.595	.506	.850	3.92	.0618	3803	.910	.820
		812	5534	63.54	.296	3310	2815	.598	.509	.851	4.22	.0664	3812	.897	.830
		812	5531	63.50	.285	3366	2860	.609	.517	.850	4.59	.0723	3858	.909	.860
		817	5522	63.22	.268	3425	2899	.620	.525	.846	4.95	.0783	3904	.938	.889
		810	5559	63.91	.264	3486	2947	.627	.530	.845	5.11	.0797	3900	.944	.907
	+4	815	5522	63.23	.314	3051	2607	.553	.472	.855	3.31	.0523	3437	.865	.700
		815	5559	63.65	.304	3138	2675	.565	.481	.853	3.57	.0561	3533	.861	.733
		814	5529	63.35	.304	3227	2735	.584	.495	.848	3.95	.0624	3661	.863	.781
		814	5523	63.28	.307	3266	2759	.591	.500	.845	4.17	.0659	3695	.862	.798
		813	5528	63.39	.300	3315	2784	.600	.504	.840	4.42	.0697	3704	.861	.813
		813	5525	63.35	.277	3355	2811	.607	.509	.838	4.71	.0743	3715	.870	.832
		812	5524	63.36	.261	3400	2842	.616	.515	.836	4.95	.0781	3742	.889	.852
50,000	0	793	4141	48.11	0.290	2434	2042	0.588	0.493	0.839	2.52	0.0524	3643	0.935	0.775
		793	4140	48.10	.292	2450	2076	.592	.502	.847	2.65	.0551	3738	.938	.805
		792	4143	48.17	.293	2466	2085	.595	.503	.846	2.80	.0581	3728	.911	.811
		792	4127	47.99	.278	2488	2114	.603	.512	.850	2.96	.0617	3822	.919	.843
		792	4138	48.11	.287	2519	2135	.609	.516	.848	3.11	.0646	3848	.915	.856
		792	4148	48.23	.286	2548	2162	.614	.521	.849	3.27	.0678	3883	.919	.875
		792	4141	48.15	.261	2606	2204	.629	.532	.846	3.47	.0721	3983	.950	.915
		792	4136	48.09	.257	2621	2208	.634	.534	.842	3.57	.0742	3979	.952	.921
		792	4147	48.22	.245	2643	2219	.637	.535	.840	3.70	.0767	3958	.953	.925
		792	4128	48.00	.271	2625	2196	.636	.532	.837	3.77	.0785	3884	.937	.914
	-4	795	4141	47.59	.302	2433	2050	.588	.495	.843	2.58	.0542	3734	.946	.788
		795	4128	47.44	.279	2440	2068	.591	.501	.848	2.73	.0575	3791	.935	.810
		794	4135	47.56	.282	2474	2095	.598	.507	.847	2.90	.0610	3832	.924	.830
		794	4149	47.72	.281	2497	2123	.602	.512	.850	3.06	.0641	3870	.923	.848
		794	4150	47.73	.284	2538	2152	.612	.519	.848	3.21	.0673	3936	.935	.873
		794	4137	47.58	.276	2561	2167	.619	.524	.846	3.35	.0704	3973	.945	.892
	+4	792	4141	48.15	.297	2435	2047	.588	.494	.841	2.58	.0536	3642	.922	.780
		792	4144	48.18	.289	2449	2078	.591	.502	.849	2.82	.0585	3699	.899	.806
		792	4137	48.10	.294	2472	2096	.598	.507	.848	2.96	.0615	3741	.895	.825
		792	4245	49.36	.295	2539	2150	.598	.507	.847	3.06	.0620	3828	.890	.823
		792	4131	48.03	.290	2491	2116	.603	.512	.850	3.08	.0641	3734	.901	.854
		792	4140	48.14	.277	2513	2134	.607	.516	.849	3.15	.0654	3796	.907	.856
		792	4164	48.42	.274	2529	2152	.607	.517	.851	3.20	.0661	3839	.909	.861
		792	4130	48.02	.261	2533	2156	.613	.522	.851	3.26	.0678	3894	.923	.879
	-7	791	4225	47.88	.339	2190	1771	.518	.419	.809	1.94	.0405	2862	.824	.529
60,000	0	788	2594	30.24	0.274	1557	1286	0.600	0.496	0.826	1.67	0.0552	3628	0.904	0.784
		788	2560	29.84	.271	1569	1301	.613	.508	.829	1.81	.0607	3755	.904	.828
		788	2653	29.88	.265	1593	1314	.622	.513	.825	1.91	.0639	3783	.899	.845
		788	2557	29.80	.265	1601	1326	.626	.519	.828	2.01	.0674	3828	.905	.866
		788	2559	29.83	.259	1603	1326	.626	.518	.827	2.10	.0704	3785	.891	.865
		788	2560	29.84	.229	1589	1318	.621	.515	.830	2.21	.0741	3683	.865	.852
		788	2553	29.76	.240	1576	1298	.617	.508	.824	2.27	.0763	3563	.834	.829
		854	2606	29.60	.323	1516	1241	.582	.476	.819	1.54	.0520	3557	.899	.703
		867	2574	29.02	.309	1518	1255	.590	.488	.827	1.72	.0593	3709	.885	.744
		870	2577	28.99	.299	1542	1279	.598	.496	.829	1.85	.0638	3811	.894	.775
		871	2581	29.03	.302	1564	1298	.606	.503	.830	1.97	.0679	3863	.900	.799
		874	2578	28.94	.299	1583	1303	.614	.505	.823	2.08	.0719	3863	.900	.808
		870	2570	28.92	.291	1597	1317	.621	.513	.825	2.17	.0750	3904	.918	.833
		868	2572	28.97	.296	1612	1319	.627	.513	.818	2.26	.0780	3855	.913	.834

[redacted]

TABLE I. - Continued. PRELIMINARY FREE-JET PERFORMANCE OF XRJ43-MA-3 RAM-JET ENGINE AT A MACH NUMBER OF 2.50

(a) Concluded. Single-pressure fuel injection

Altitude, ft	Angle of attack, α, deg	Free-stream total temperature, T_0, °R	Free-stream total pressure, P_0, lb/sq ft abs	Combustor supercritical air flow, $W_{a,5}$, lb/sec	Diffuser outlet Mach number, M_2	Diffuser outlet total pressure, P_2, lb/sq ft abs	Exhaust nozzle total pressure, P_5, lb/sq ft abs	Diffuser total pressure recovery, $\frac{P_2}{P_0}$	Engine total pressure ratio, $\frac{P_5}{P_0}$	Combustor total pressure ratio, $\frac{P_5}{P_2}$	Fuel flow, W_f, lb/sec	Fuel air ratio, $\frac{W_f}{W_{a,5}}$	Exhaust gas total temperature, T_5, °R	Combustion efficiency, η_b	Net thrust coefficient, C_{F_n}
60,000	-4	788	2576	29.74	0.299	1479	1202	0.574	0.467	0.813	1.50	0.0504	3320	0.852	0.688
		788	2597	29.99	.297	1529	1251	.589	.482	.818	1.57	.0524	3519	.896	.740
		788	2576	29.74	.283	1538	1264	.597	.491	.822	1.66	.0558	3619	.896	.773
		788	2573	29.71	.280	1545	1271	.601	.494	.823	1.72	.0579	3643	.887	.783
		788	2572	29.70	.276	1557	1285	.605	.500	.825	1.78	.0599	3708	.894	.804
		866	2581	28.79	.322	1483	1215	.575	.471	.819	1.54	.0535	3589	.893	.691
		866	2577	28.75	.316	1498	1239	.581	.481	.827	1.70	.0591	3684	.878	.727
		866	2579	28.77	.304	1518	1257	.589	.487	.828	1.81	.0629	3745	.878	.751
		866	2578	28.76	.300	1541	1275	.598	.495	.827	1.90	.0661	3819	.891	.777
		866	2584	28.82	.304	1566	1289	.606	.499	.823	2.00	.0694	3844	.895	.792
		866	2575	28.73	.298	1574	1298	.611	.504	.825	2.11	.0734	3868	.905	.810
	+4	777	2540	29.79	.353	1247	1032	.491	.406	.828	1.30	.0436	2489	.641	.464
		780	2580	30.20	.347	1360	1109	.527	.430	.815	1.37	.0454	2780	.725	.548
		775	2575	30.25	.328	1323	1105	.514	.429	.835	1.40	.0463	2744	.704	.546
		770	2599	30.62	.317	1355	1138	.521	.438	.840	1.45	.0474	2830	.722	.577
		786	2584	30.12	.312	1505	1221	.582	.473	.811	1.46	.0485	3361	.890	.701
		786	2579	30.07	.302	1516	1237	.588	.480	.816	1.53	.0509	3436	.886	.726
		775	2621	30.79	.302	1548	1271	.591	.485	.821	1.60	.0520	3448	.880	.746
		784	2582	30.14	.301	1539	1260	.596	.488	.819	1.60	.0531	3525	.891	.757
		867	2587	29.13	.307	1474	1223	.570	.473	.830	1.55	.0532	3555	.884	.691
		855	2580	29.25	.296	1509	1254	.585	.486	.831	1.70	.0581	3658	.879	.739
		868	2561	28.82	.282	1508	1253	.589	.489	.831	1.79	.0621	3720	.873	.751
		881	2557	28.56	.290	1536	1272	.601	.498	.828	1.93	.0676	3834	.890	.780
		880	2578	28.81	.287	1552	1291	.602	.501	.832	2.01	.0698	3855	.896	.792
		880	2576	28.79	.288	1556	1294	.604	.502	.832	2.07	.0719	3849	.895	.797
65,000	0	792	1997	23.22	0.339	1138	913	0.570	0.457	0.802	1.27	0.0547	3105	0.740	0.646
		793	2016	23.42	.301	1217	993	.604	.493	.816	1.31	.0559	3598	.887	.772
		791	2018	23.48	.303	1245	1020	.617	.506	.819	1.39	.0592	3743	.909	.819
		790	2020	23.51	.288	1268	1038	.628	.514	.819	1.50	.0638	3814	.908	.849
		790	2016	23.47	.276	1279	1049	.634	.520	.820	1.60	.0680	3858	.912	.872
		789	2015	23.47	.278	1282	1052	.636	.522	.821	1.70	.0724	3819	.902	.878
		789	2018	23.51	.266	1253	1034	.621	.512	.825	1.80	.0766	3622	.852	.844
	+4	791	2035	23.66	.334	1143	928	.562	.456	.812	1.27	.0537	3099	.738	.642
		791	2037	23.68	.297	1227	1007	.602	.494	.821	1.34	.0564	3614	.888	.780
		791	2043	23.75	.301	1249	1021	.611	.500	.818	1.40	.0589	3668	.887	.799
		792	2019	23.46	.286	1247	1023	.618	.507	.820	1.47	.0625	3733	.888	.824
		792	2032	23.61	.285	1259	1033	.620	.508	.821	1.50	.0635	3748	.889	.830
		792	2038	23.67	.282	1267	1039	.622	.510	.820	1.54	.0649	3756	.887	.835
		876	2034	22.78	.326	1143	949	.562	.467	.830	1.19	.0522	3511	.927	.669
		877	2030	22.73	.297	1181	976	.582	.481	.826	1.35	.0592	3655	.867	.720
		874	2035	22.82	.276	1203	1002	.591	.492	.833	1.44	.0631	3782	.886	.762
		873	2036	22.84	.272	1220	1013	.599	.498	.830	1.54	.0675	3808	.884	.780
		873	2033	22.81	.272	1237	1025	.609	.504	.829	1.65	.0723	3839	.893	.804
		872	2035	22.84	.262	1247	1025	.613	.504	.822	1.75	.0766	3770	.881	.802

3635

TABLE I. - Continued. PRELIMINARY FREE-JET PERFORMANCE OF XRJ43-MA-3 RAM-JET ENGINE AT A MACH NUMBER OF 2.50

(b) Inner-ring-only fuel injection

Altitude, ft	Angle of attack, α, deg	Free-stream total temperature, T_0, °R	Free-stream total pressure, P_0, lb/sq ft abs	Combustor supercritical air flow, $W_{a,5}$, lb/sec	Diffuser outlet Mach number, M_2	Diffuser outlet total pressure, P_2, lb/sq ft abs	Exhaust nozzle total pressure, P_5, lb/sq ft abs	Diffuser total pressure recovery, $\frac{P_2}{P_0}$	Engine total pressure ratio, $\frac{P_5}{P_0}$	Combustor total pressure ratio, $\frac{P_5}{P_2}$	Fuel flow, W_f, lb/sec	Fuel air ratio, $\frac{W_f}{W_{a,5}}$	Exhaust gas total temperature, T_5, °R	Combustion efficiency, η_b	Net thrust coefficient, C_{F_n}
44,000	+4	811	5521	63.37	0.466	2325	1875	0.421	0.340	0.807	1.86	0.0294	1899	0.565	0.224
		811	5527	63.44	.423	2515	2078	.455	.376	.826	2.15	.0339	2293	.685	.355
		812	5523	63.35	.392	2644	2215	.479	.401	.838	2.41	.0380	2580	.744	.445
		812	5527	63.40	.375	2749	2318	.497	.419	.843	2.68	.0423	2784	.760	.511
		812	5525	63.37	.357	2815	2379	.510	.431	.845	2.90	.0458	2904	.757	.551
		908	5502	60.54	.406	2587	2156	.470	.392	.833	2.31	.0382	2675	.748	.401
45,000	+4	816	5316	60.83	0.372	2541	2092	0.478	0.394	0.823	2.24	0.0367	2489	0.725	0.407
		819	5299	60.53	.363	2547	2099	.481	.396	.824	2.27	.0375	2539	.732	.416
50,000	0	794	4124	47.88	0.433	1759	1433	0.427	0.348	0.815	1.43	0.0299	1940	0.586	0.252
		790	4117	47.92	.398	1901	1569	.462	.381	.825	1.66	.0345	2285	.679	.373
		790	4122	47.98	.376	1980	1646	.480	.399	.831	1.81	.0377	2484	.716	.438
		790	4119	47.94	.356	2080	1722	.505	.418	.828	2.05	.0427	2684	.722	.506
		789	4118	47.97	.335	2126	1767	.516	.429	.831	2.22	.0463	2790	.716	.545
	-4	787	4124	47.65	.451	1775	1416	.430	.343	.798	1.45	.0304	1910	.566	.245
		787	4117	47.57	.429	1904	1543	.463	.375	.810	1.65	.0347	2243	.659	.357
		780	4116	47.76	.403	2021	1662	.491	.404	.822	1.83	.0382	2553	.740	.461
		796	4158	47.77	.383	2101	1732	.505	.417	.824	2.01	.0420	2738	.751	.507
		782	4122	47.78	.381	2118	1754	.514	.426	.828	2.07	.0433	2797	.759	.539
		775	4179	48.65	.365	2190	1807	.524	.432	.825	2.21	.0453	2846	.751	.564
		776	4115	47.87	.358	2186	1818	.531	.442	.832	2.27	.0474	2955	.765	.597
	+4	790	4119	47.90	0.423	1744	1430	0.423	0.347	0.820	1.44	0.0301	1929	0.579	0.252
		787	4123	48.05	.383	1898	1567	.460	.380	.826	1.68	.0349	2266	.666	.370
		786	4118	48.01	.357	1977	1637	.480	.398	.828	1.83	.0382	2452	.696	.432
		782	4121	48.18	.347	2068	1720	.502	.417	.832	2.05	.0425	2652	.715	.504
		784	4130	48.22	.339	2118	1758	.513	.426	.830	2.21	.0458	2738	.704	.534
60,000	0	786	2580	30.11	0.436	1087	886	0.421	0.343	0.815	0.92	0.0304	1872	0.547	0.237
		785	2580	30.13	.410	1143	944	.443	.366	.826	1.03	.0340	2097	.604	.318
		784	2582	30.17	.381	1217	1014	.471	.393	.833	1.18	.0391	2376	.652	.414
		782	2574	30.12	.360	1258	1052	.489	.409	.836	1.28	.0425	2536	.671	.471
		784	2647	30.93	.359	1314	1106	.496	.418	.842	1.37	.0443	2645	.688	.504
		780	2560	29.99	.329	1345	1119	.525	.437	.832	1.46	.0487	2846	.711	.574
	-4	788	2575	29.73	.466	1091	871	.424	.338	.798	.93	.0313	1848	.522	.226
		785	2574	29.77	.441	1136	921	.441	.358	.811	1.02	.0343	2041	.574	.296
		785	2581	29.85	.413	1217	991	.472	.384	.814	1.18	.0394	2316	.623	.390
		785	2583	29.88	.396	1247	1024	.483	.396	.821	1.25	.0418	2447	.645	.435
		786	2582	29.84	.378	1299	1075	.503	.416	.828	1.39	.0466	2667	.670	.506
		874	2590	28.77	.481	1071	849	.414	.328	.793	.85	.0295	1886	.526	.178
		874	2584	28.70	.427	1146	920	.444	.356	.803	.99	.0345	2191	.603	.279
		871	2587	28.78	.415	1189	965	.460	.373	.812	1.10	.0380	2371	.635	.341
		878	2587	28.66	.398	1246	1017	.482	.393	.816	1.23	.0429	2615	.668	.413
		878	2589	28.69	.377	1304	1071	.504	.414	.821	1.35	.0469	2861	.712	.487
	+4	785	2574	30.03	.441	1066	864	.414	.336	.811	.91	.0303	1790	.508	.211
		785	2573	30.02	.379	1196	994	.465	.386	.831	1.16	.0386	2308	.631	.392
		785	2572	30.01	.364	1235	1022	.480	.397	.828	1.26	.0420	2417	.631	.432
		786	2576	30.03	.349	1271	1051	.493	.408	.827	1.35	.0450	2528	.637	.470
		867	2584	29.10	.441	1074	873	.416	.338	.813	.89	.0306	1943	.543	.208
		868	2582	29.05	.396	1132	930	.438	.360	.822	.99	.0341	2189	.611	.288
		873	2577	28.91	.386	1179	977	.458	.379	.829	1.10	.0380	2410	.651	.356
		871	2572	28.89	.355	1231	1018	.479	.396	.827	1.21	.0419	2588	.671	.415
		867	2572	28.96	.351	1271	1050	.494	.408	.826	1.33	.0458	2708	.671	.460
65,000	0	784	2029	23.71	0.447	834	673	0.411	0.332	0.807	0.72	0.0303	1742	0.484	0.195
		786	2022	23.59	.411	883	724	.437	.358	.820	.82	.0347	2007	.552	.290
		787	2052	23.94	.381	936	775	.456	.378	.828	.92	.0383	2209	.593	.360
		786	2046	23.88	.382	962	796	.470	.389	.827	1.00	.0419	2316	.592	.401
		788	2033	23.70	.349	1013	836	.498	.411	.825	1.10	.0464	2557	.632	.480
	+4	788	2029	23.63	.463	812	656	.400	.323	.808	.70	.0296	1670	.454	.166
		788	2028	23.62	.409	884	728	.436	.359	.824	.82	.0348	2025	.558	.294
		791	2032	23.62	.399	913	752	.449	.370	.824	.89	.0377	2140	.570	.334
		790	2045	23.78	.373	963	796	.471	.389	.827	.99	.0417	2336	.601	.402
		788	2041	23.77	.369	1003	823	.491	.403	.821	1.10	.0463	2465	.600	.453
		873	2041	22.89	.403	917	750	.450	.368	.818	.86	.0376	2267	.595	.314

TABLE I. - Continued. PRELIMINARY FREE-JET PERFORMANCE OF XRJ43-MA-3 RAM-JET ENGINE AT A MACH NUMBER OF 2.50

(c) Dual-pressure fuel injection

Altitude, ft	Angle of attack, α, deg	Free-stream total temperature, T_0, °R	Free-stream total pressure, P_0, lb/sq ft abs	Combustor supercritical air flow, $W_{a,5}$, lb/sec	Diffuser outlet Mach number, M_2	Diffuser outlet total pressure, P_2, lb/sq ft abs	Exhaust nozzle total pressure, P_5, lb/sq ft abs	Diffuser total pressure recovery, $\frac{P_2}{P_0}$	Engine total pressure ratio, $\frac{P_5}{P_0}$	Combustor total pressure ratio, $\frac{P_5}{P_2}$	Fuel flow, W_f, lb/sec	Fuel air ratio, $\frac{W_f}{W_{a,5}}$	Exhaust gas total temperature, T_5, °R	Combustion efficiency, η_b	Net thrust coefficient, C_{F_n}
44,000	+4	811	5521	63.37	0.380	2693	2269	0.488	0.411	0.843	2.56	[a]0.0403	2686	0.751	0.481
		811	5530	63.47	.335	2941	2534	.532	.458	.862	3.10	[a].0488	3254	.843	.650
		811	5523	63.40	.306	3114	2684	.564	.486	.862	3.52	[a].0554	3593	.886	.752
		811	5526	63.43	.305	3224	2766	.583	.501	.858	3.87	[a].0609	3754	.899	.802
		811	5525	63.42	.360	2804	2388	.508	.432	.852	2.81	.0443	2933	.788	.557
		811	5525	63.42	.327	2950	2548	.534	.461	.864	3.22	.0508	3278	.828	.661
		811	5522	63.38	.299	3143	2701	.569	.489	.859	3.69	.0581	3613	.872	.761
		811	5528	63.45	.306	3239	2769	.586	.501	.855	4.03	.0634	3733	.881	.803
		811	5521	63.37	.304	3306	2807	.599	.508	.849	4.41	.0696	3769	.881	.830
		921	5546	60.57	.375	2740	2317	.494	.418	.846	2.67	.0438	3029	.801	.494
		927	5534	60.25	.346	2867	2452	.518	.443	.855	3.04	.0505	3365	.836	.585
		922	5555	60.65	.328	2980	2569	.537	.463	.862	3.40	.0560	3589	.859	.655
		927	5516	60.05	.311	3042	2617	.552	.474	.860	3.73	.0620	3737	.869	.697
		918	5511	60.29	.313	3093	2646	.561	.480	.856	4.04	.0669	3732	.854	.718
45,000	+4	817	5274	60.32	0.256	3256	2693	0.617	0.511	0.827	3.85	0.0638	3900	0.930	0.827
		814	5282	60.52	.258	3325	2743	.630	.519	.825	4.18	.0691	3955	.936	.858
50,000	-4	787	4127	47.68	0.401	2005	1637	0.486	0.397	0.817	2.09	0.0439	2441	0.617	0.436
		789	4130	47.65	.302	2383	1959	.577	.474	.822	2.40	.0503	3435	.892	.715
		797	4181	48.00	.290	2441	2025	.584	.484	.830	2.68	.0558	3566	.877	.751
		791	4132	47.62	.288	2448	2023	.593	.490	.826	2.69	.0564	3607	.886	.769
		787	4111	47.50	.334	2225	1822	.541	.443	.819	2.80	.0589	2924	.659	.603
		785	4162	48.14	.303	2303	1900	.553	.457	.825	2.98	.0620	3067	.691	.650
		783	4124	47.77	.296	2401	1971	.582	.478	.821	3.30	.0691	3278	.740	.727
	+4	783	4116	48.09	.317	2228	1839	.541	.447	.825	1.97	[a].0410	3057	.895	.609
		777	4093	48.01	.309	2405	1963	.588	.480	.816	2.26	[a].0471	3432	.937	.727
		785	4095	47.78	.288	2472	2043	.604	.499	.827	2.57	[a].0538	3682	.935	.796
		793	4140	48.06	.277	2493	2076	.602	.502	.833	2.71	[a].0563	3731	.925	.806
		795	4134	47.92	.274	2510	2090	.607	.506	.833	2.82	[a].0588	3780	.922	.820
		789	4123	47.98	.311	2296	1898	.557	.460	.827	2.19	.0456	3225	.882	.658
		787	4136	48.20	.312	2418	1990	.585	.481	.823	2.43	.0504	3464	.901	.732
		786	4135	48.21	.290	2501	2062	.605	.499	.825	2.65	.0550	3672	.920	.795
		785	4144	48.35	.282	2476	2060	.598	.497	.832	2.70	.0558	3637	.902	.790
		785	4135	48.24	.274	2477	2068	.599	.500	.835	2.74	.0568	3671	.905	.800
		787	4139	48.24	.272	2494	2086	.603	.504	.836	2.85	.0591	3710	.900	.814
		786	4126	48.10	.269	2520	2112	.611	.512	.838	2.97	.0617	3796	.912	.842
60,000	0	785	2579	30.12	0.328	1335	1097	0.518	0.425	0.822	1.23	[a]0.0409	2773	0.785	0.532
		783	2578	30.15	.291	1495	1235	.580	.479	.826	1.46	[a].0484	3432	.916	.725
		781	2580	30.20	.274	1552	1289	.602	.500	.831	1.68	[a].0557	3647	.906	.797
		781	2580	30.20	.265	1592	1316	.617	.510	.827	1.86	[a].0616	3741	.896	.835
		787	2579	30.08	.380	1212	1000	.470	.388	.825	1.35	.0449	2284	.548	.396
		788	2582	30.10	.293	1484	1227	.575	.475	.827	1.52	.0505	3377	.870	.711
		784	2581	30.16	.280	1547	1280	.599	.496	.827	1.71	.0567	3599	.882	.784
		783	2581	30.18	.265	1594	1324	.618	.513	.831	1.89	.0628	3779	.902	.846
		783	2582	30.19	.248	1624	1354	.629	.524	.834	2.08	.0689	3874	.917	.886
	-4	789	2584	29.81	.406	1204	970	.466	.375	.806	1.20	[a].0403	2218	.571	.359
		787	2585	29.87	.326	1466	1187	.567	.459	.810	1.39	[a].0464	3246	.879	.660
		789	2576	29.72	.374	1302	1091	.505	.424	.838	1.38	[a].0465	2770	.707	.532
		787	2586	29.88	.326	1407	1174	.544	.454	.834	1.56	[a].0523	3123	.767	.641
		787	2577	29.78	.311	1527	1237	.593	.480	.810	1.57	[a].0527	3487	.883	.735
		792	2579	29.70	.311	1560	1264	.605	.490	.810	1.69	[a].0570	3618	.885	.771
		790	2576	29.70	.294	1581	1286	.614	.499	.813	1.81	[a].0609	3702	.887	.804
		758	2588	30.47	.387	1295	1062	.500	.410	.820	1.33	.0436	2517	.657	.484
		786	2580	29.82	.381	1280	1045	.496	.405	.816	1.34	.0450	2534	.639	.465
		786	2582	29.84	.321	1392	1148	.539	.445	.825	1.37	.0460	3049	.814	.607
		783	2576	29.84	.348	1370	1146	.532	.445	.837	1.48	.0496	3006	.755	.608
		786	2583	29.86	.344	1365	1133	.529	.439	.830	1.52	.0510	2924	.714	.586

[a]Inner ring fuel-air ratio, 0.033 - All others, 0.037.

TABLE I. - Concluded. PRELIMINARY FREE-JET PERFORMANCE OF XRJ43-MA-3 RAM-JET ENGINE AT A MACH NUMBER OF 2.50

(c) Concluded. Dual-pressure fuel injection

Altitude, ft	Angle of attack, α, deg	Free-stream total temperature, T_0, °R	Free-stream total pressure, P_0, lb/sq ft abs	Combustor supercritical air flow, $W_{a,5}$, lb/sec	Diffuser outlet Mach number, M_2	Diffuser outlet total pressure, P_2, lb/sq ft abs	Exhaust nozzle total pressure, P_5, lb/sq ft abs	Diffuser total pressure recovery, $\frac{P_2}{P_0}$	Engine total pressure ratio, $\frac{P_5}{P_0}$	Combustor total pressure ratio, $\frac{P_5}{P_2}$	Fuel flow, W_f, lb/sec	Fuel air ratio, $\frac{W_f}{W_{a,5}}$	Exhaust gas total temperature, T_5, °R	Combustion efficiency, η_b	Net thrust coefficient, C_{F_n}
60,000	-4	786	2583	29.86	0.315	1501	1223	0.581	0.474	0.815	1.55	0.0518	3395	0.862	0.711
		786	2572	29.73	.326	1422	1192	.553	.464	.838	1.60	.0538	3238	.792	.675
		787	2567	29.66	.304	1452	1221	.566	.476	.841	1.68	.0566	3386	.816	.718
		786	2584	29.87	.308	1557	1264	.603	.489	.812	1.71	.0571	3574	.872	.768
		786	2584	29.87	.303	1440	1209	.557	.468	.840	1.72	.0574	3264	.773	.691
		793	2566	29.53	.309	1561	1266	.608	.493	.811	1.72	.0582	3657	.857	.782
		775	2593	30.19	.295	1600	1308	.617	.504	.818	1.80	.0596	3721	.903	.822
		870	2583	28.75	.419	1180	962	.457	.372	.815	1.26	.0440	2318	.545	.339
		870	2587	28.79	.360	1328	1100	.513	.425	.828	1.44	.0501	2969	.718	.528
		875	2580	28.63	.327	1412	1159	.547	.449	.821	1.45	.0507	3329	.834	.613
		869	2594	28.89	.323	1405	1168	.542	.450	.831	1.62	.0560	3270	.767	.618
		867	2581	28.78	.319	1480	1208	.573	.468	.816	1.62	.0564	3522	.846	.682
		868	2587	28.83	.308	1513	1248	.585	.482	.825	1.78	.0619	3689	.865	.733
		878	2583	28.62	.309	1558	1277	.603	.494	.820	1.97	.0687	3834	.890	.777
	+4	786	2578	30.06	.312	1336	1108	.518	.430	.829	1.26	a.0420	2831	.790	.548
		786	2572	29.99	.311	1467	1207	.570	.469	.823	1.44	a.0480	3315	.881	.690
		785	2579	30.09	.291	1541	1261	.598	.489	.818	1.66	a.0550	3524	.873	.761
		770	2572	30.30	.320	1406	1159	.547	.451	.824	1.32	.0436	3032	.846	.622
		786	2577	30.04	.304	1366	1131	.530	.439	.828	1.33	.0442	2933	.796	.581
		785	2575	30.04	.345	1266	1043	.492	.405	.824	1.33	.0444	2494	.632	.460
		771	2594	30.54	.320	1494	1228	.576	.473	.822	1.46	.0478	3311	.885	.705
		786	2571	29.97	.320	1332	1117	.518	.435	.839	1.51	.0502	2823	.687	.565
		785	2577	30.06	.320	1488	1223	.577	.475	.822	1.53	.0509	3361	.861	.709
		769	2564	30.23	.307	1522	1244	.594	.485	.817	1.55	.0513	3432	.883	.747
		767	2580	30.46	.304	1545	1263	.599	.490	.818	1.58	.0519	3480	.893	.762
		769	2589	30.52	.303	1554	1272	.600	.491	.819	1.64	.0537	3499	.880	.769
		786	2583	30.11	.288	1541	1271	.597	.492	.825	1.69	.0560	3564	.877	.772
		786	2562	29.87	.293	1401	1180	.547	.461	.842	1.69	.0564	3119	.734	.659
		873	2577	28.91	.428	1227	988	.476	.383	.805	1.31	.0452	2409	.566	.371
		878	2577	28.83	.320	1400	1157	.543	.449	.826	1.45	.0503	3274	.818	.606
		874	2573	28.85	.321	1321	1101	.513	.428	.834	1.48	.0513	2951	.699	.531
		877	2576	28.84	.309	1467	1209	.570	.469	.824	1.62	.0561	3515	.844	.680
		879	2580	28.85	.295	1505	1245	.583	.483	.827	1.79	.0622	3665	.854	.726
		871	2584	29.03	.293	1561	1286	.604	.498	.824	1.98	.0681	3788	.878	.781
65,000	0	787	2045	23.86	0.361	987	823	0.483	0.402	0.834	1.05	.0439	2463	0.625	0.449
		792	2030	23.60	.315	1190	978	.586	.482	.822	1.19	.0506	3490	.906	.733
		789	2037	23.73	.298	1238	1020	.608	.501	.824	1.33	.0560	3697	.918	.801
		788	2039	23.77	.294	1273	1045	.624	.513	.821	1.48	.0623	3797	.909	.844
		788	2026	23.62	.282	1285	1054	.634	.520	.820	1.62	.0687	3837	.906	.871
	+4	790	1997	23.22	.385	936	766	.469	.384	.818	.97	a.0416	2269	.576	.382
		790	2032	23.63	.337	1161	958	.571	.472	.825	1.14	a.0483	3363	.892	.698
		790	2030	23.61	.298	1220	1002	.601	.494	.821	1.31	a.0554	3612	.896	.777
		790	2032	23.63	.296	1256	1029	.618	.506	.819	1.45	a.0614	3737	.895	.823
		788	2028	23.62	.354	998	827	.492	.408	.829	1.04	.0442	2538	.649	.469
		788	2024	23.57	.320	1171	970	.579	.479	.828	1.20	.0507	3439	.889	.726
		789	2021	23.52	.298	1218	1004	.603	.497	.824	1.33	.0565	3642	.897	.788
		790	2021	23.50	.300	1256	1030	.622	.510	.820	1.48	.0631	3769	.897	.835
		790	2019	23.48	.288	1195	1002	.592	.496	.839	1.57	.0670	3530	.816	.787
		873	2029	22.76	.367	981	809	.484	.399	.825	1.00	.0440	2616	.656	.426
		873	2028	22.75	.308	1099	919	.542	.453	.836	1.14	.0502	3318	.835	.621
		873	2028	22.75	.316	1154	953	.569	.470	.826	1.28	.0561	3509	.842	.681
		873	2031	22.78	.302	1189	984	.585	.485	.828	1.41	.0620	3674	.858	.733
		873	2029	22.76	.292	1222	1011	.602	.498	.827	1.55	.0680	3811	.884	.783

[a]Inner ring fuel-air ratio, 0.033 - All others, 0.037.

3635

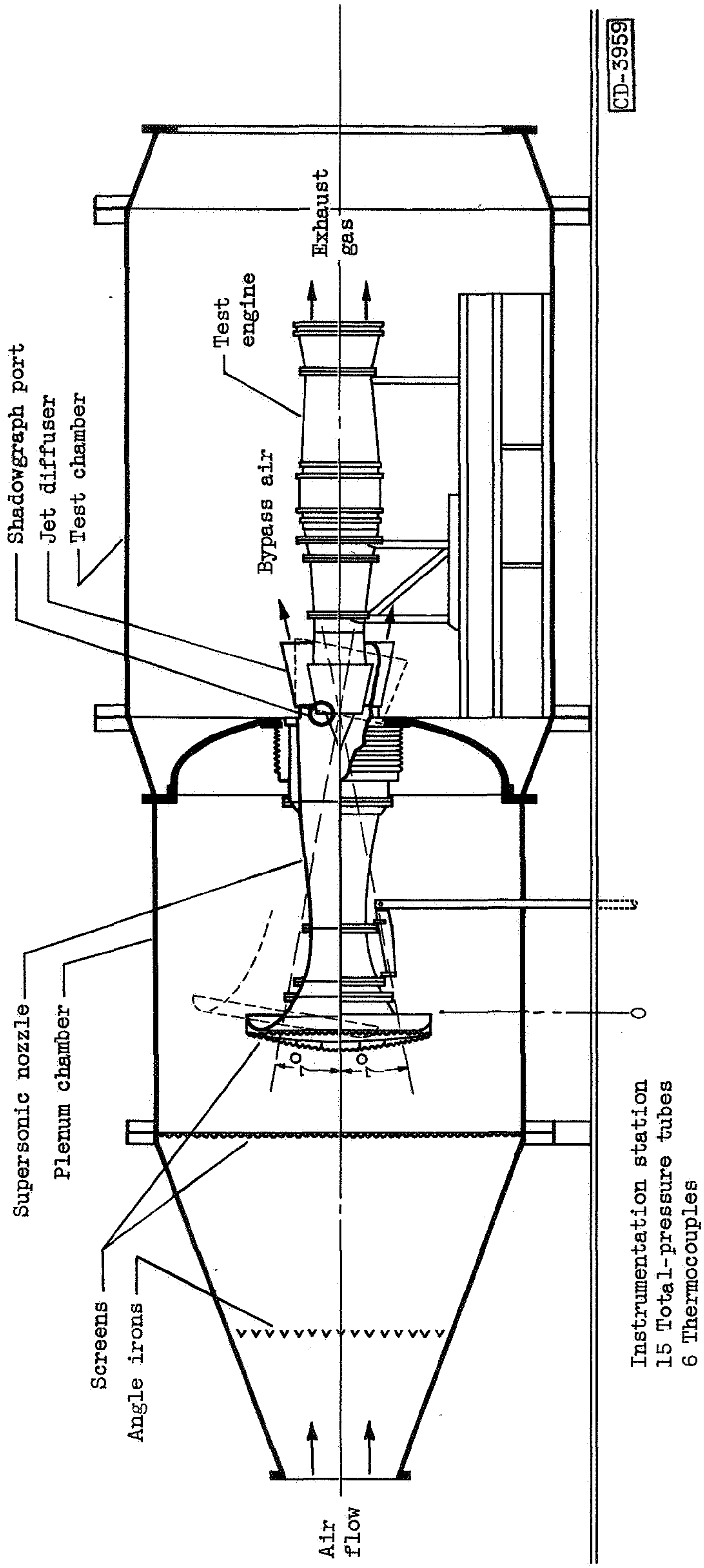

Figure 1. - Installation of XRJ43-MA-3 ram-jet engine in altitude test chamber.

3635

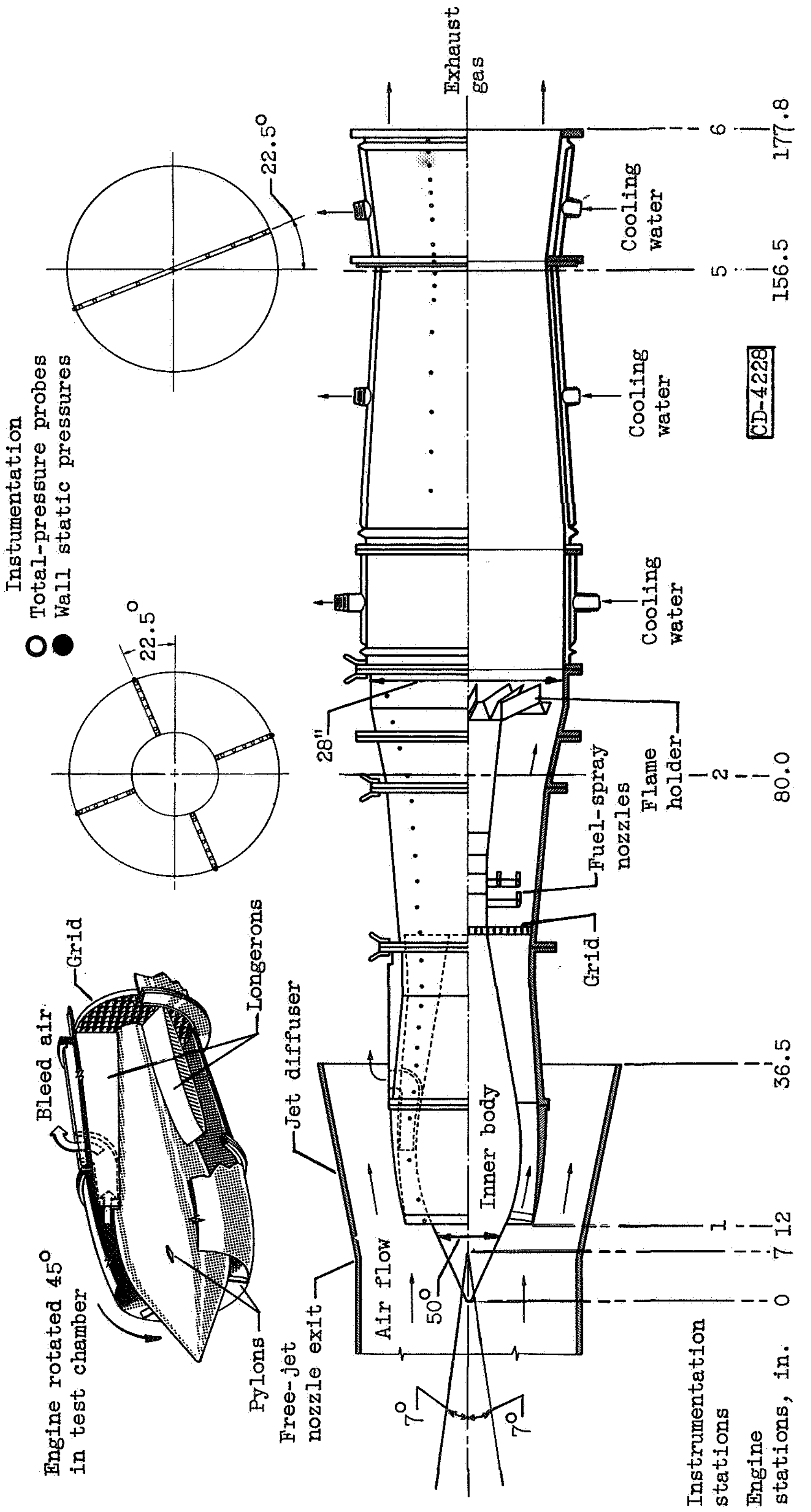

Figure 2. - Cross-sectional view of XRJ43-MA-3 ram-jet engine.

[redacted]

3635

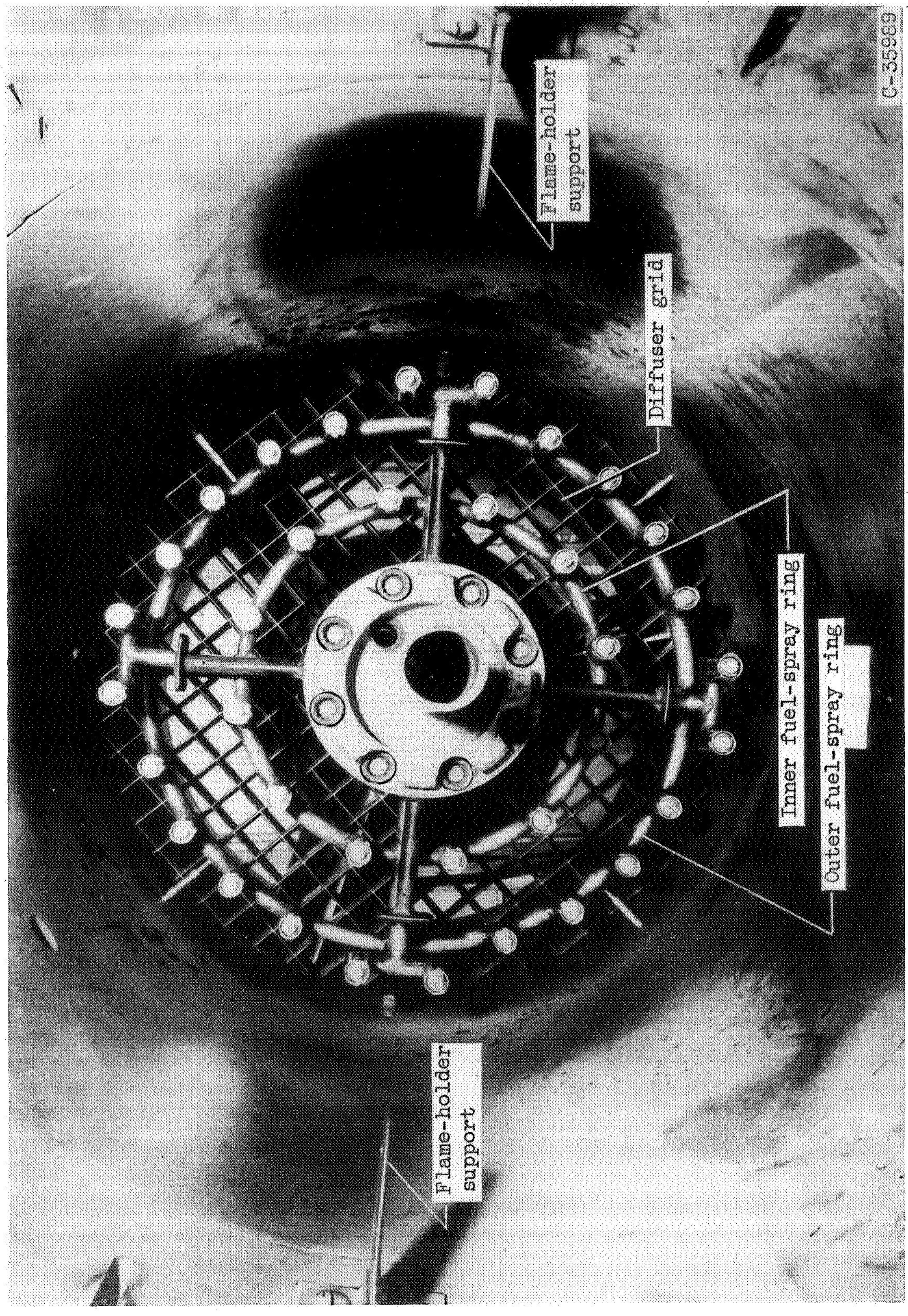

Figure 3. - View looking upstream showing fuel-spray rings and grid installed in diffuser. Flame holder removed.

3635

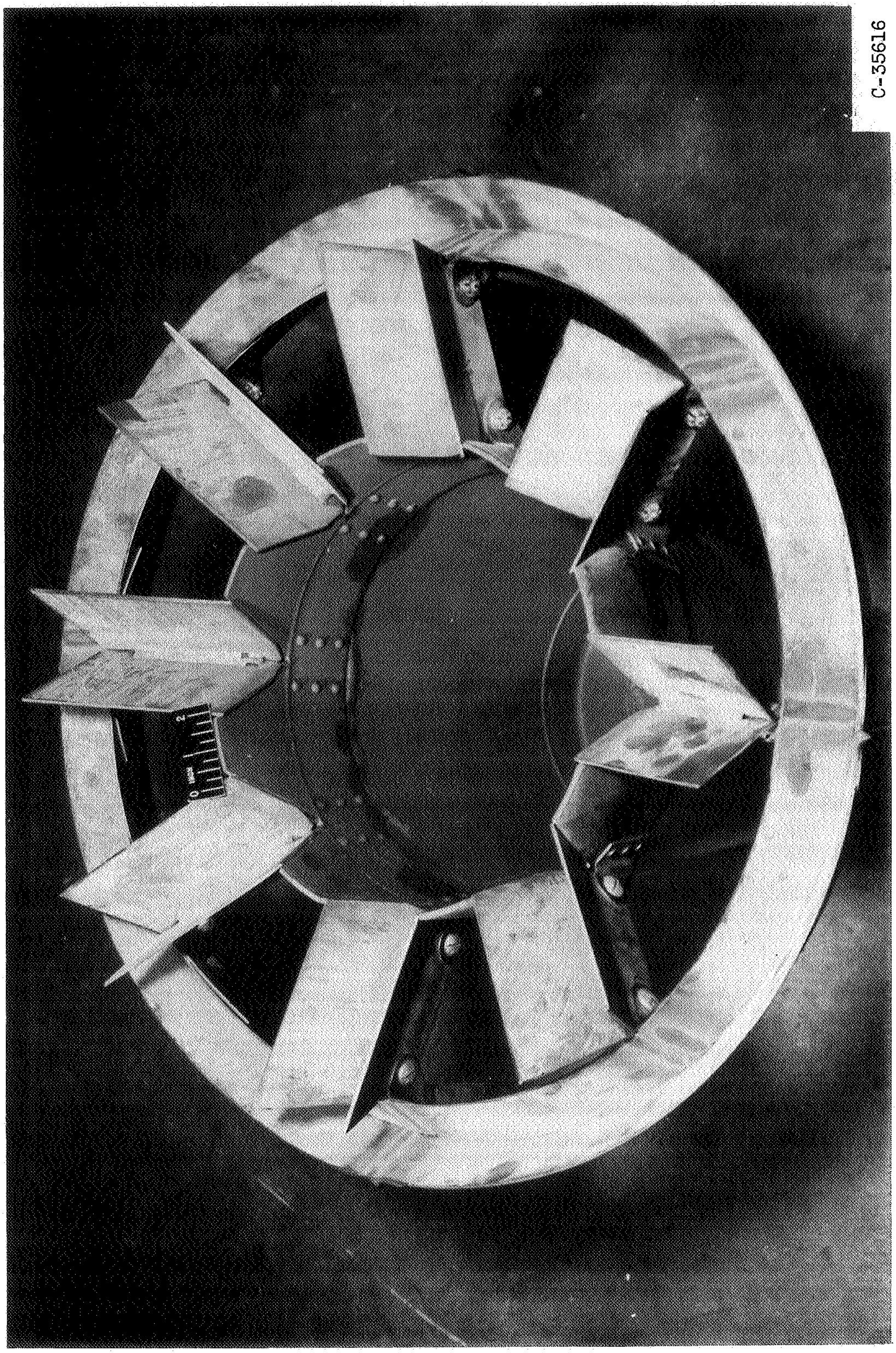

(a) Three-quarter view of downstream face.

Figure 4. - Flame holder used in XRJ43-MA-3 model 20B3 ram-jet engine.

[redacted]

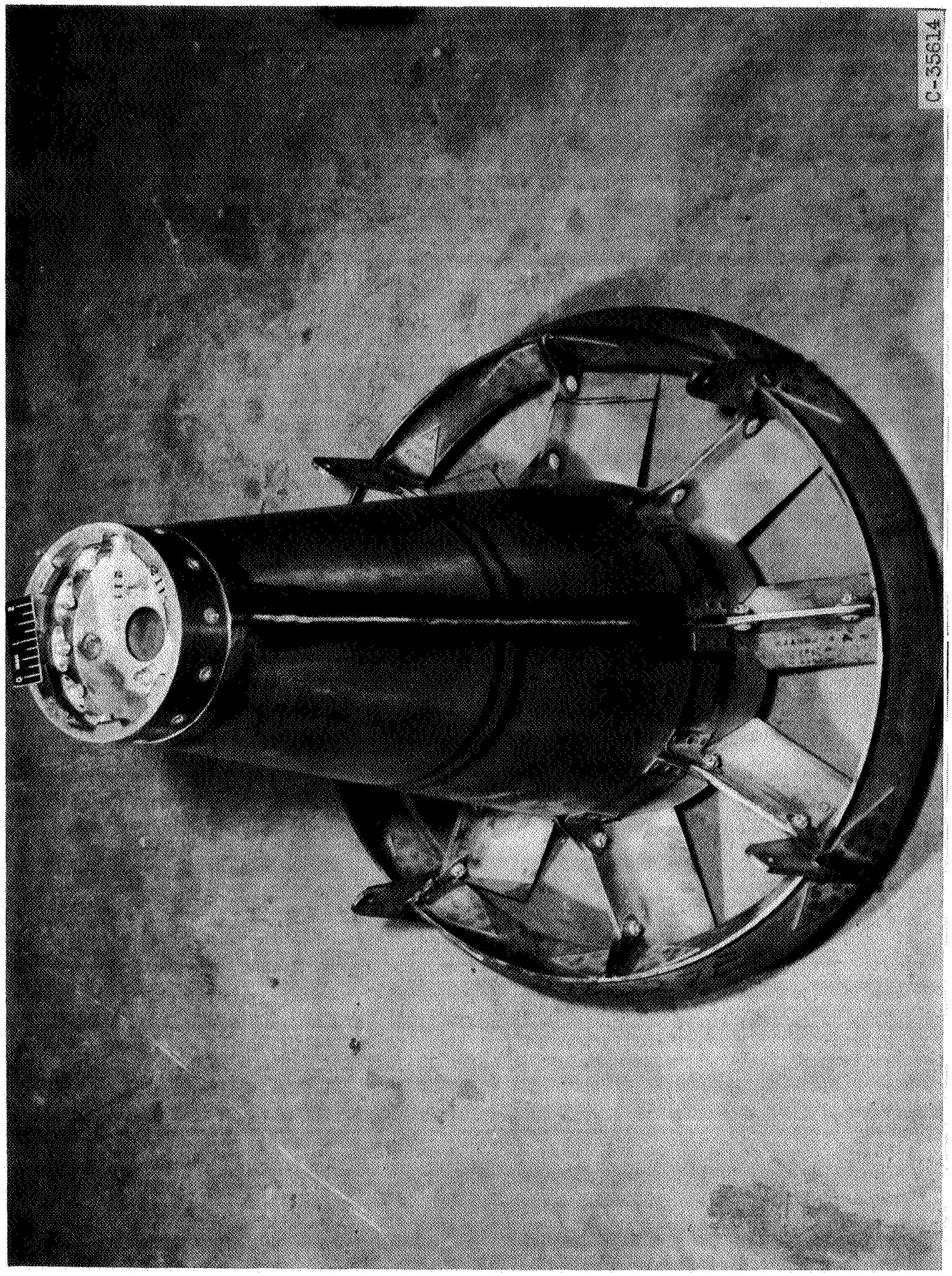

(b) Three-quarter view of upstream face.

Figure 4. - Concluded. Flame holder used in XRJ43-MA-3 model 20B3 ram-jet engine.

3635

DECLASSIFIED

3635

CX-4

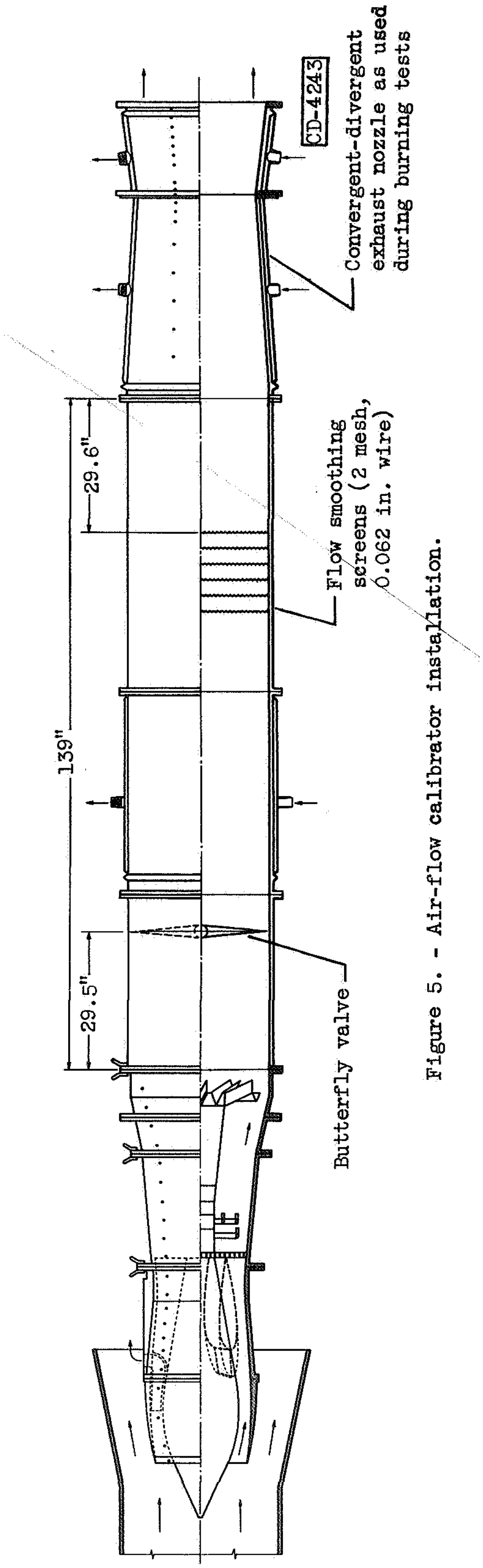

Figure 5. - Air-flow calibrator installation.

[redacted]

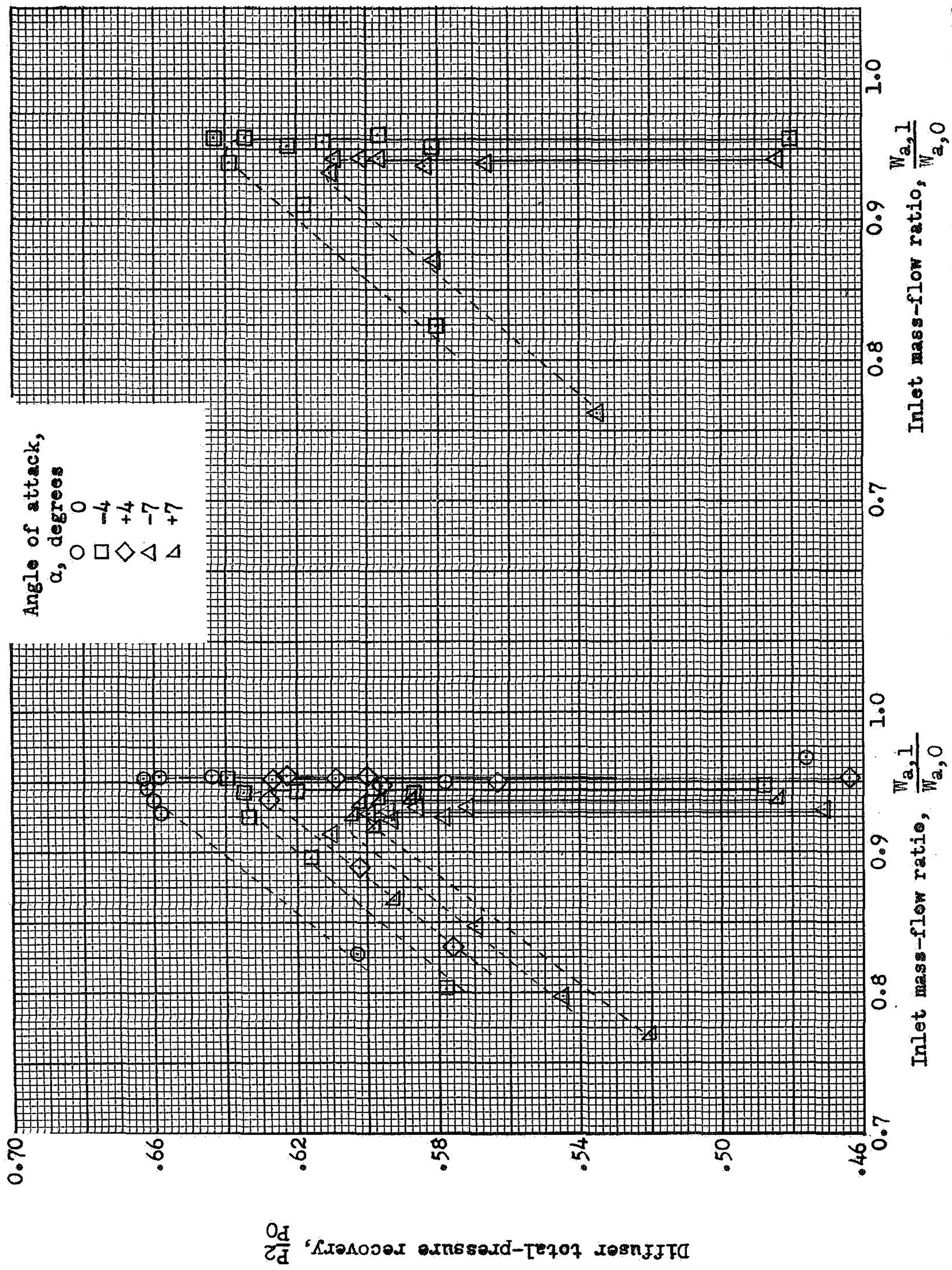

(a) Miami cold day inlet temperature, 790 °R. (b) Miami hot day inlet temperature, 873 °R.

Figure 6. - Inlet-air-flow calibration. Altitude, 60,000 feet.

3635

DECLASSIFIED

3635 CX-4 back

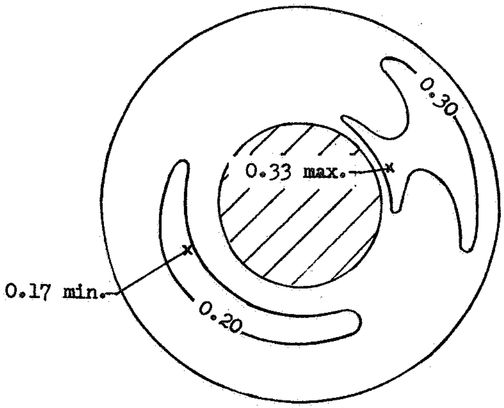

Diffuser total-pressure recovery, 0.658.

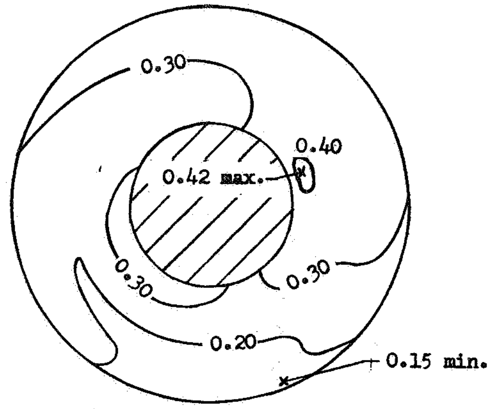

Diffuser total-pressure recovery, 0.578.

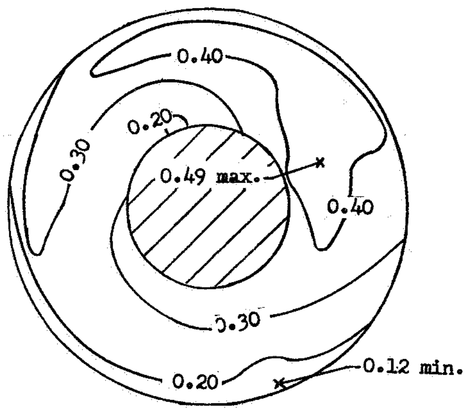

Diffuser total-pressure recovery, 0.525.

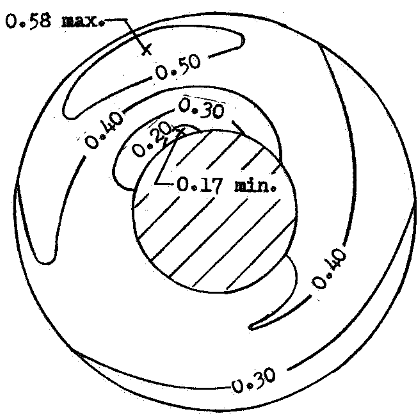

Diffuser total-pressure recovery, 0.476.

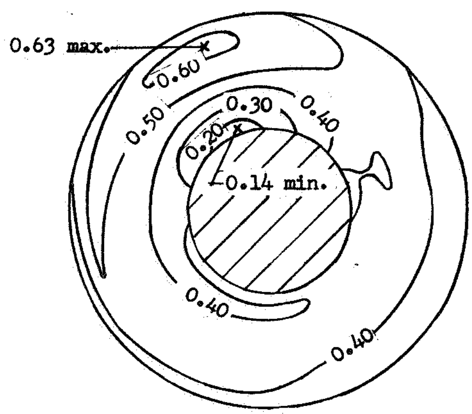

Diffuser total-pressure recovery, 0.421.

(a) Effect of diffuser total-pressure recovery. Angle of attack, α, 0°.

Figure 7. - Diffuser-outlet (station 2) Mach number contours. Altitude, 60,000 feet; inlet temperature, 790 °R (MCD).

[redacted]

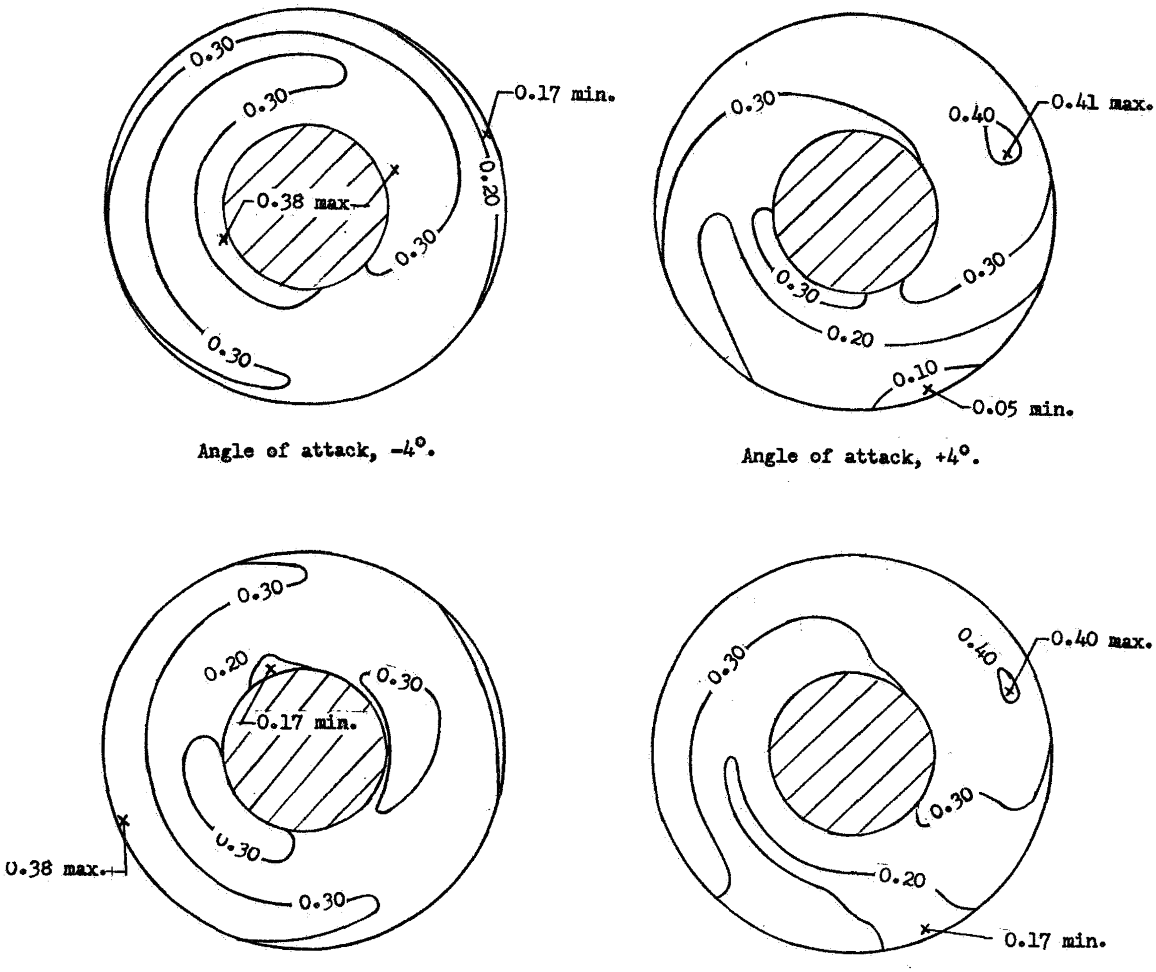

Angle of attack, -4°.

Angle of attack, +4°.

Angle of attack, -7°.

Angle of attack, +7°.

(b) Effect of angle of attack. Diffuser total-pressure recovery, approximately 0.595.

Figure 7. - Diffuser-outlet (station 2) Mach number contours. Altitude, 60,000 feet; inlet temperature, 790 °R (MCD).

[redacted]

3635

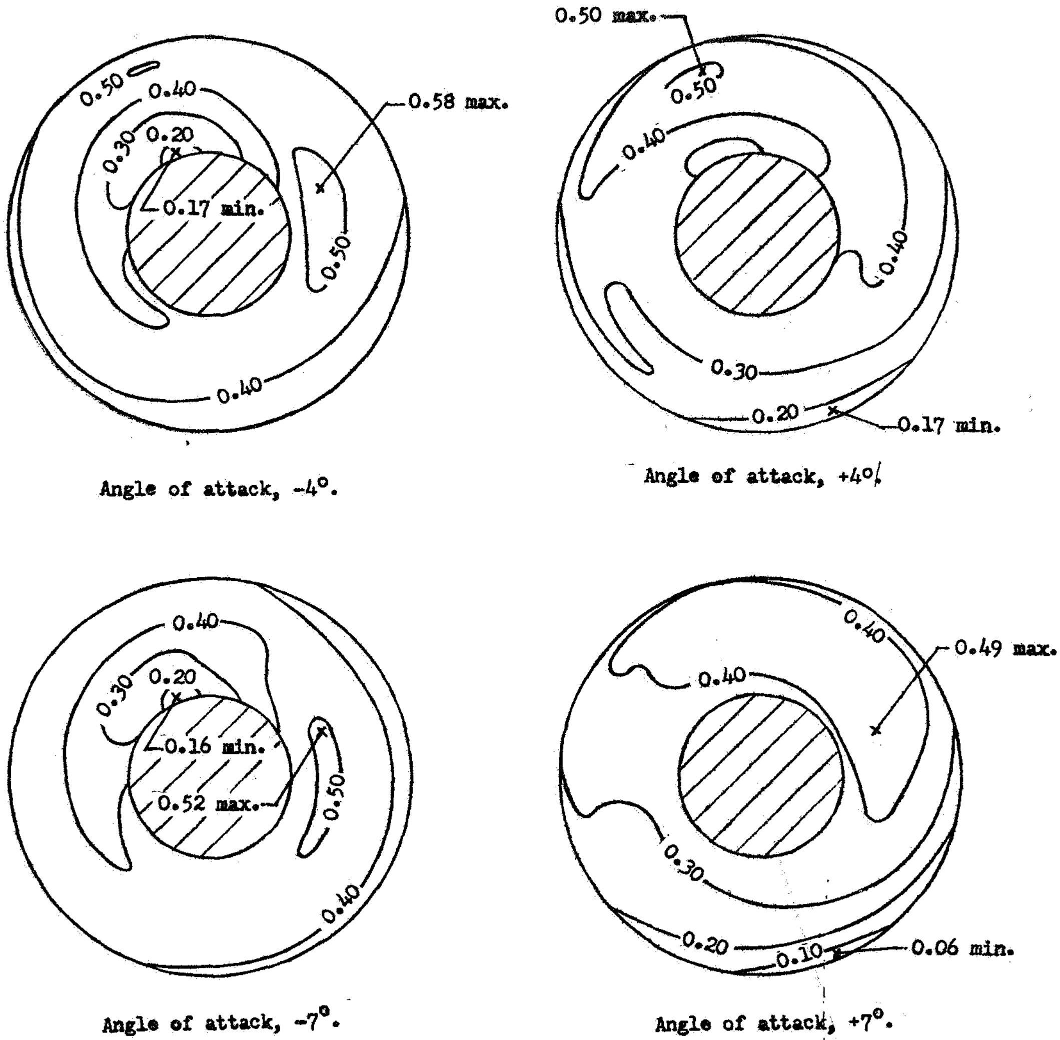

(c) Effect of angle of attack. Diffuser total pressure recovery, approximately 0.475.

Figure 7. - Diffuser outlet (station 2) Mach number contours. Altitude, 60,000 feet; inlet temperature, 790 °R (MCD).

[redacted]

3635

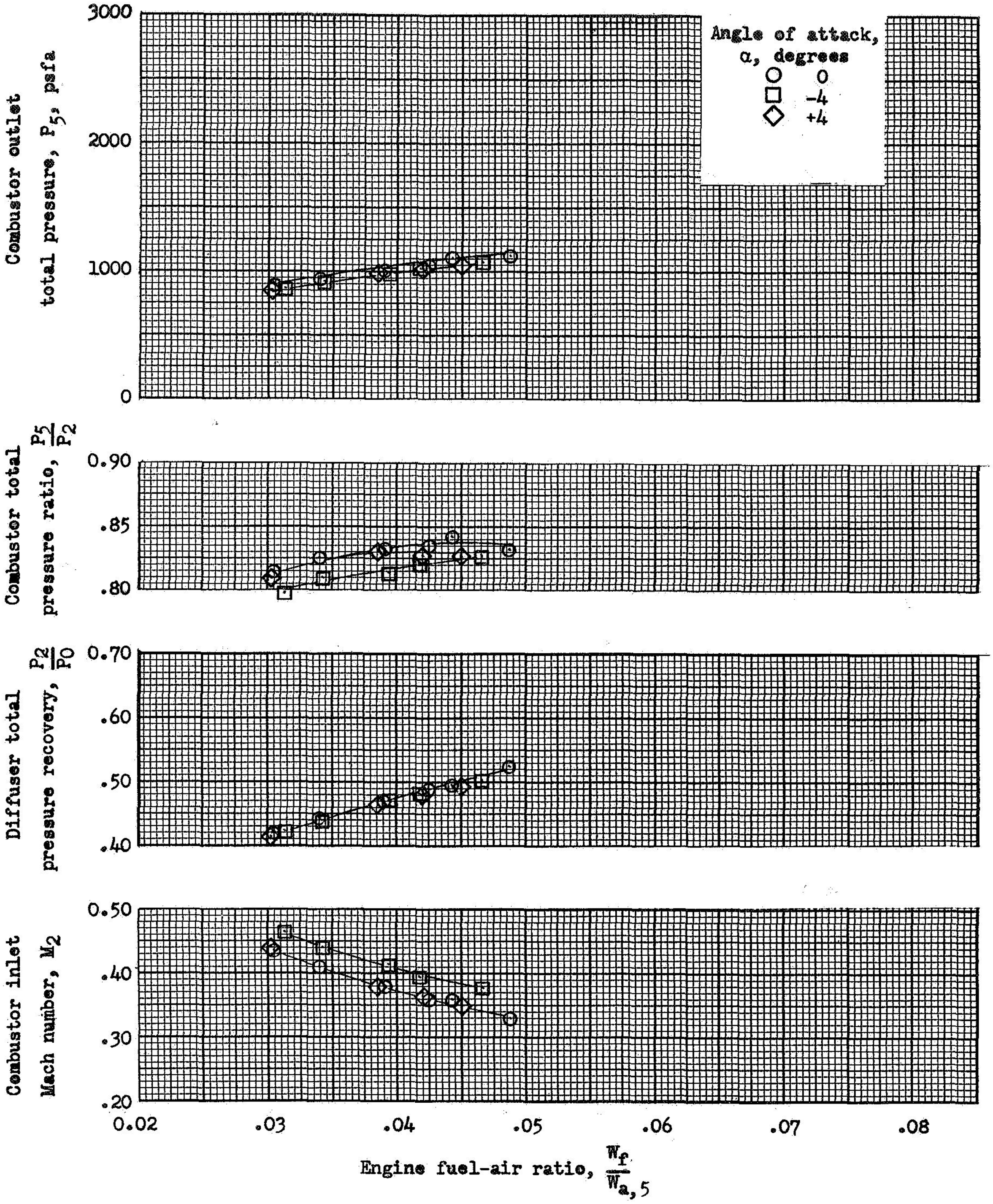

(a) Inner-ring-only fuel injection.

Figure 8. - Engine performance. Altitude, 60,000 feet; inlet temperature, 790 °R (MCD).

[redacted]

DECLASSIFIED

3635

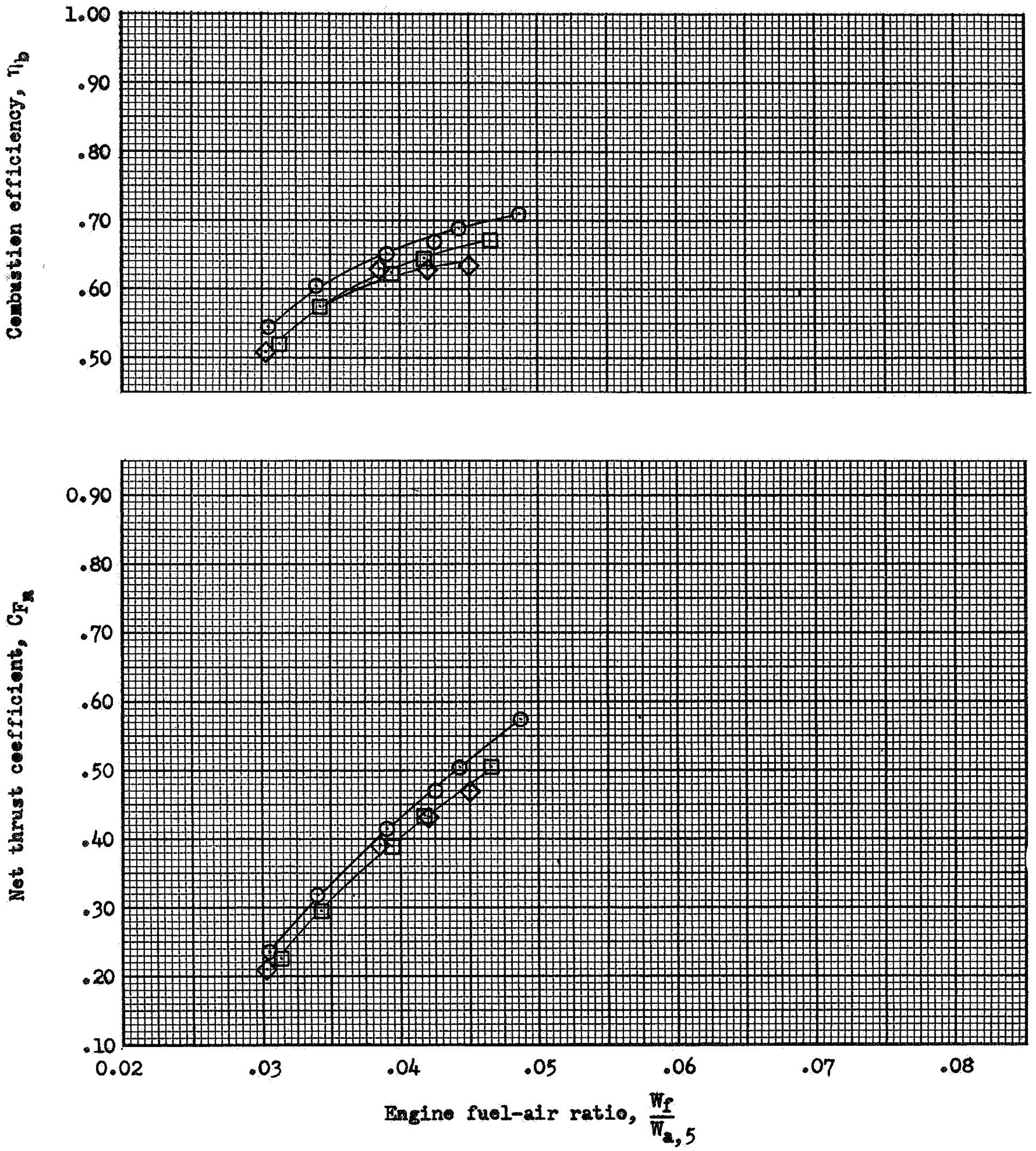

(a) Concluded. Inner-ring-only fuel injection.

Figure 8. - Continued. Engine performance. Altitude, 60,000 feet; inlet temperature, 790° R (MCD).

3635

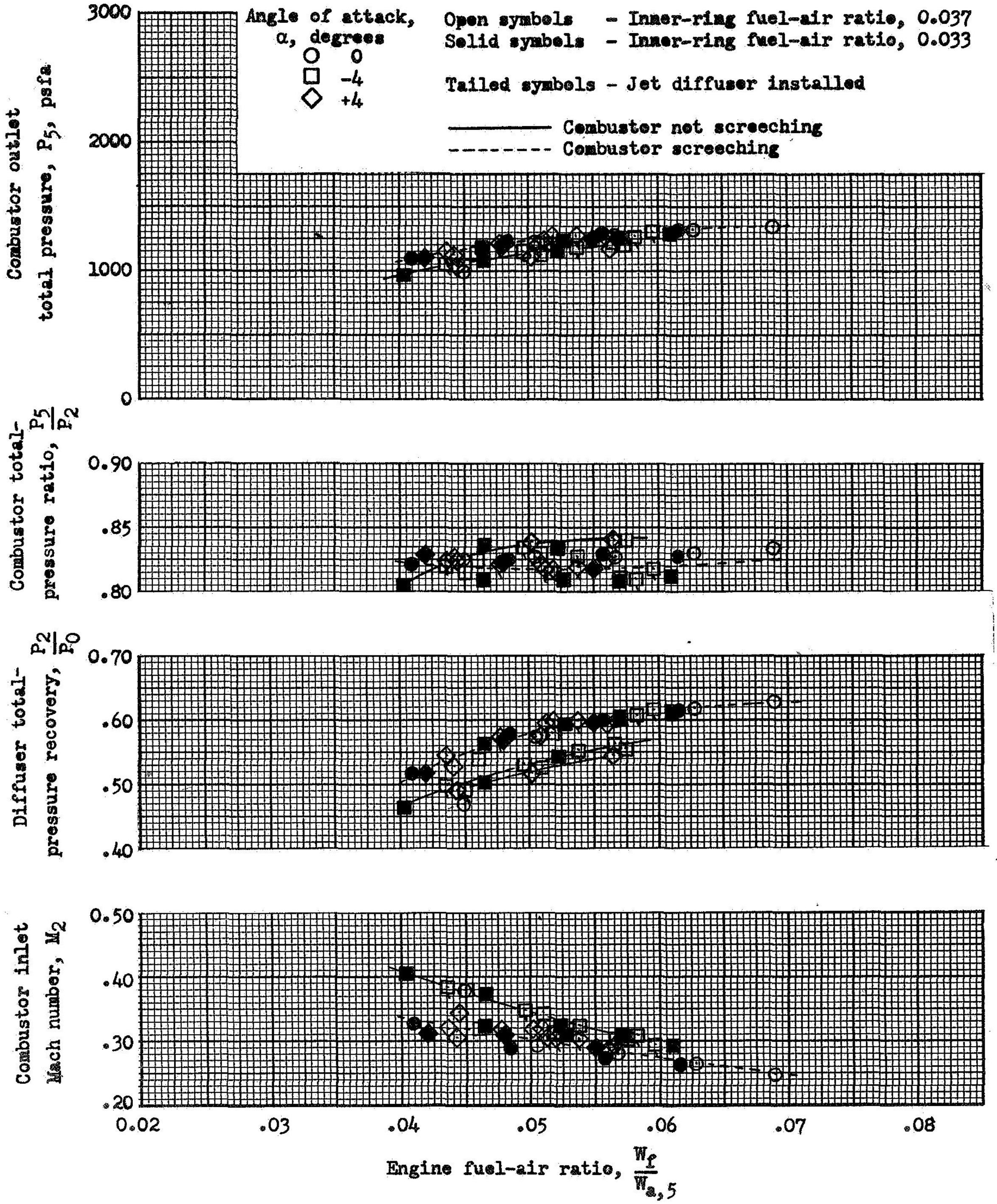

(b) Dual-pressure fuel injection

Figure 8. - Continued. Engine performance. Altitude, 60,000 feet; inlet temperature, 790 °R (MCD).

[redacted]

DECLASSIFIED

3635

CX-5

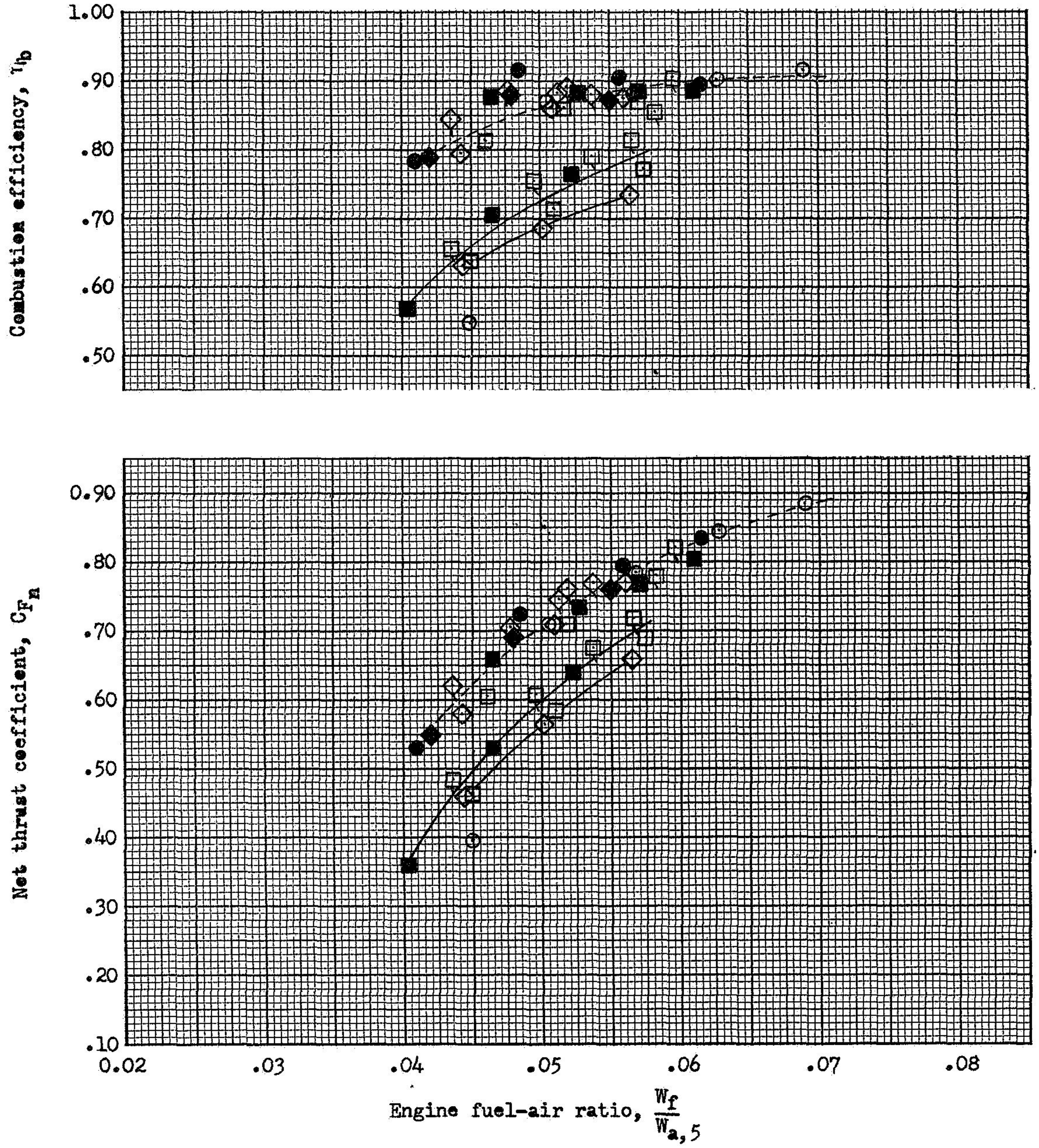

(b) Concluded. Dual-pressure fuel injection.

Figure 8. - Continued. Engine performance. Altitude, 60,000 feet; inlet temperature, 790° R (MCD).

[redacted]

3635

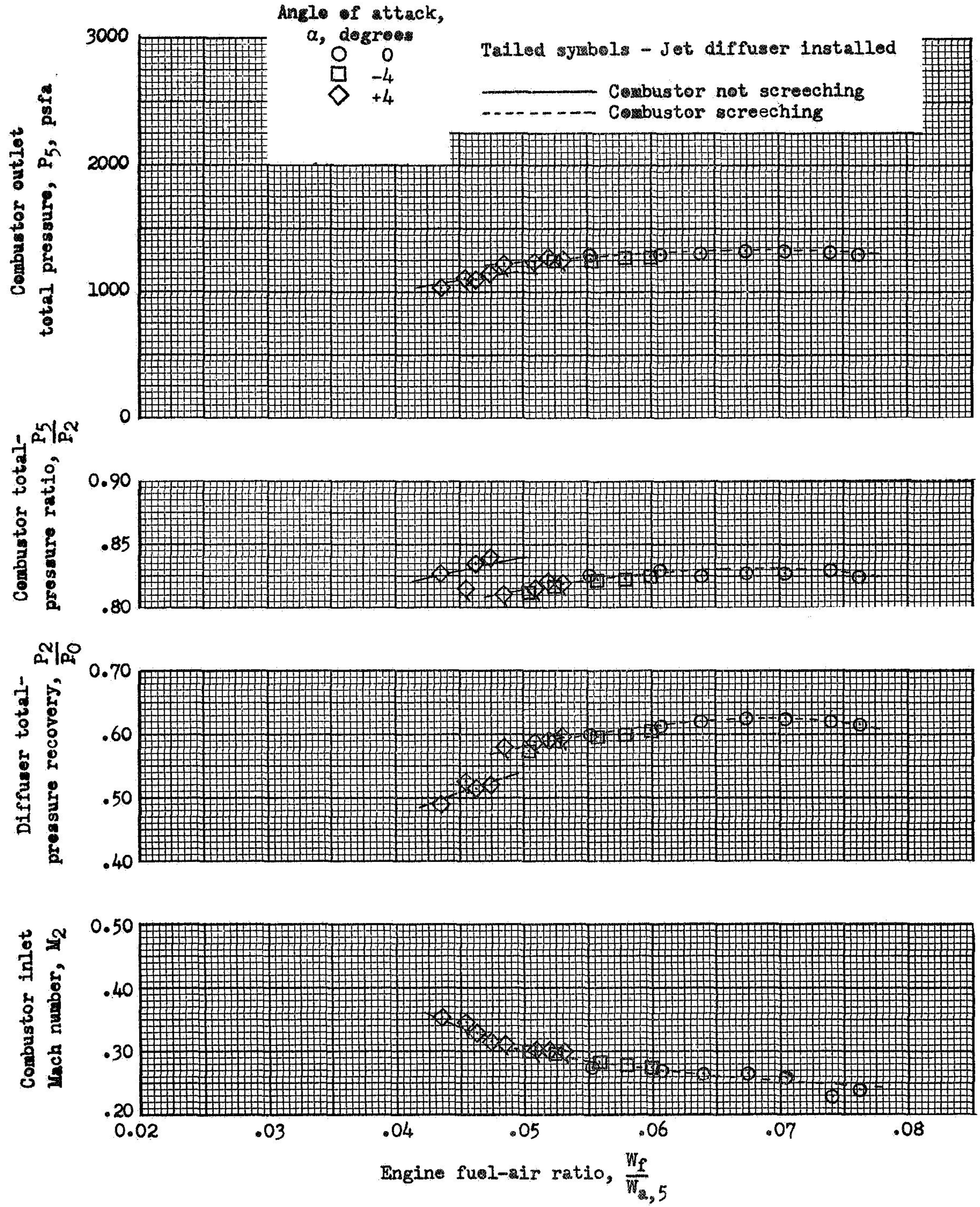

(c) Single-pressure fuel injection

Figure 8. - Continued. Engine performance. Altitude, 60,000 feet; inlet temperature, 790 °R (MCD).

[redacted]

DECLASSIFIED

3635

CX-5 back

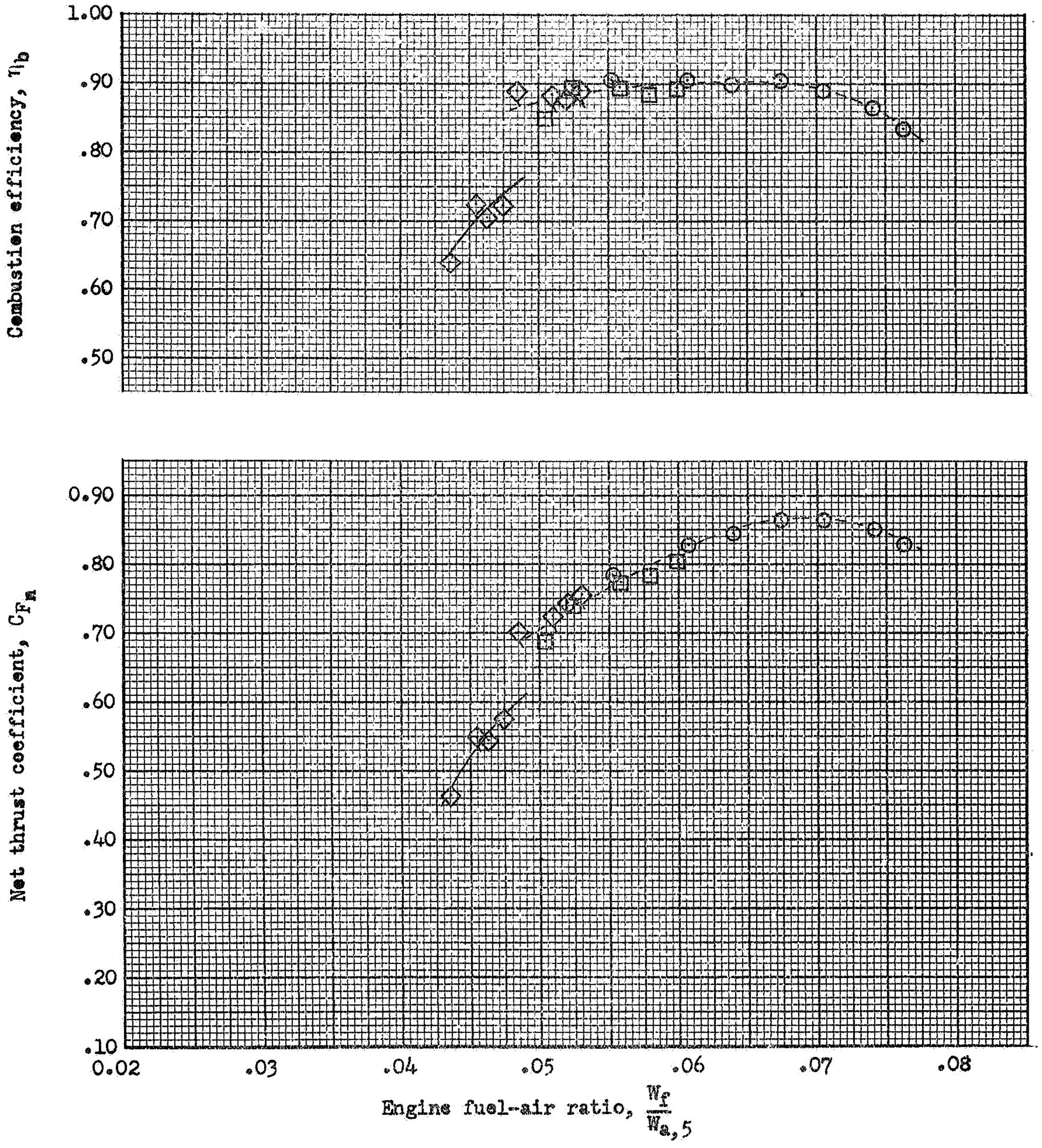

(c) Concluded. Single-pressure fuel injection.

Figure 8. - Concluded. Engine performance. Altitude, 60,000 feet; inlet temperature, 790° R (MCD).

3635

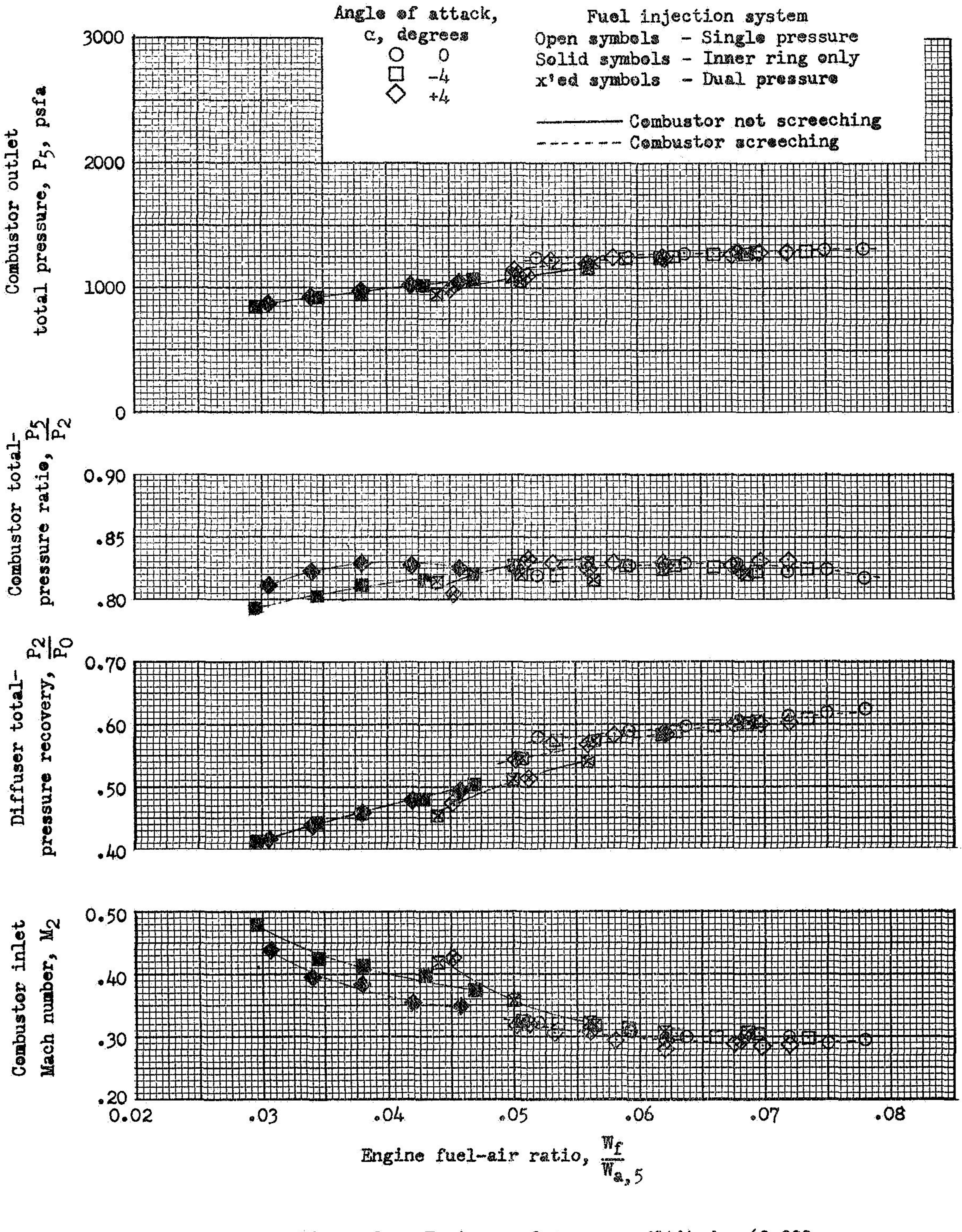

Figure 9. - Engine performance. Altitude, 60,000 feet; inlet temperature, 873 °R (MHD).

DECLASSIFIED

3635

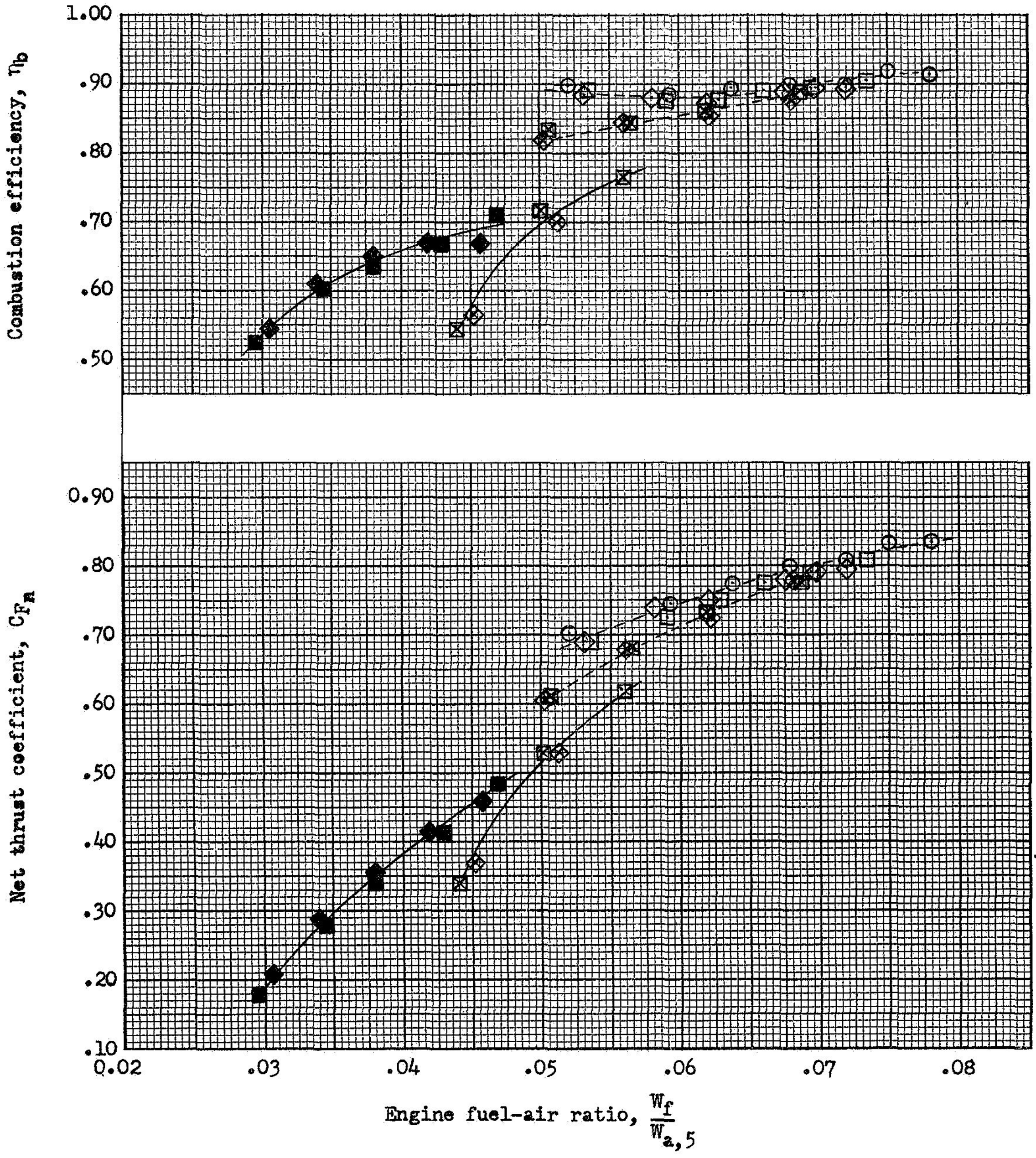

Figure 9. - Concluded. Engine performance. Altitude, 60,000 feet; inlet temperature, 873 °R (MHD).

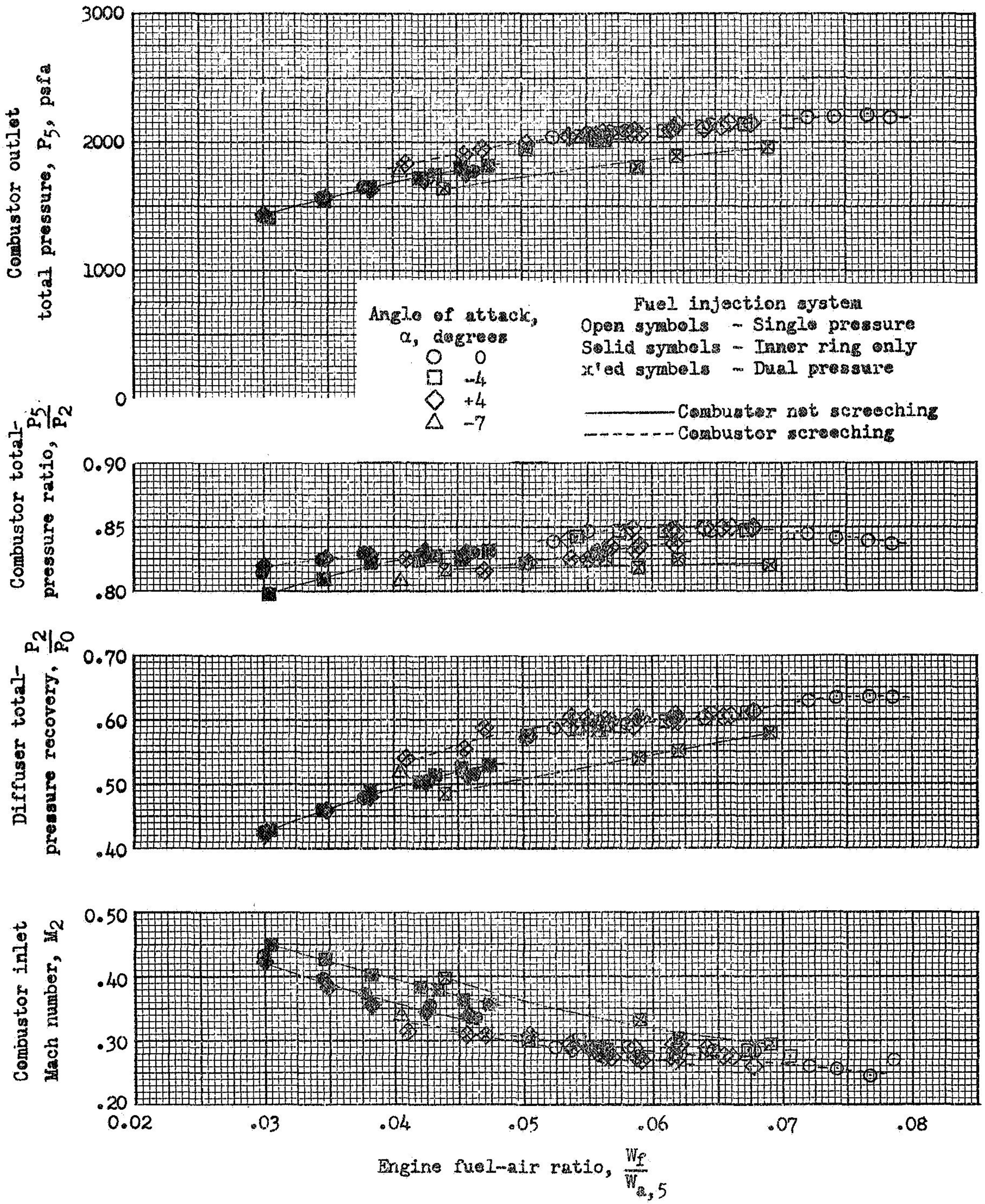

Figure 10. - Engine performance. Altitude, 50,000 feet; inlet temperature, 790 °R (MCD).

[redacted]

DECLASSIFIED

3635

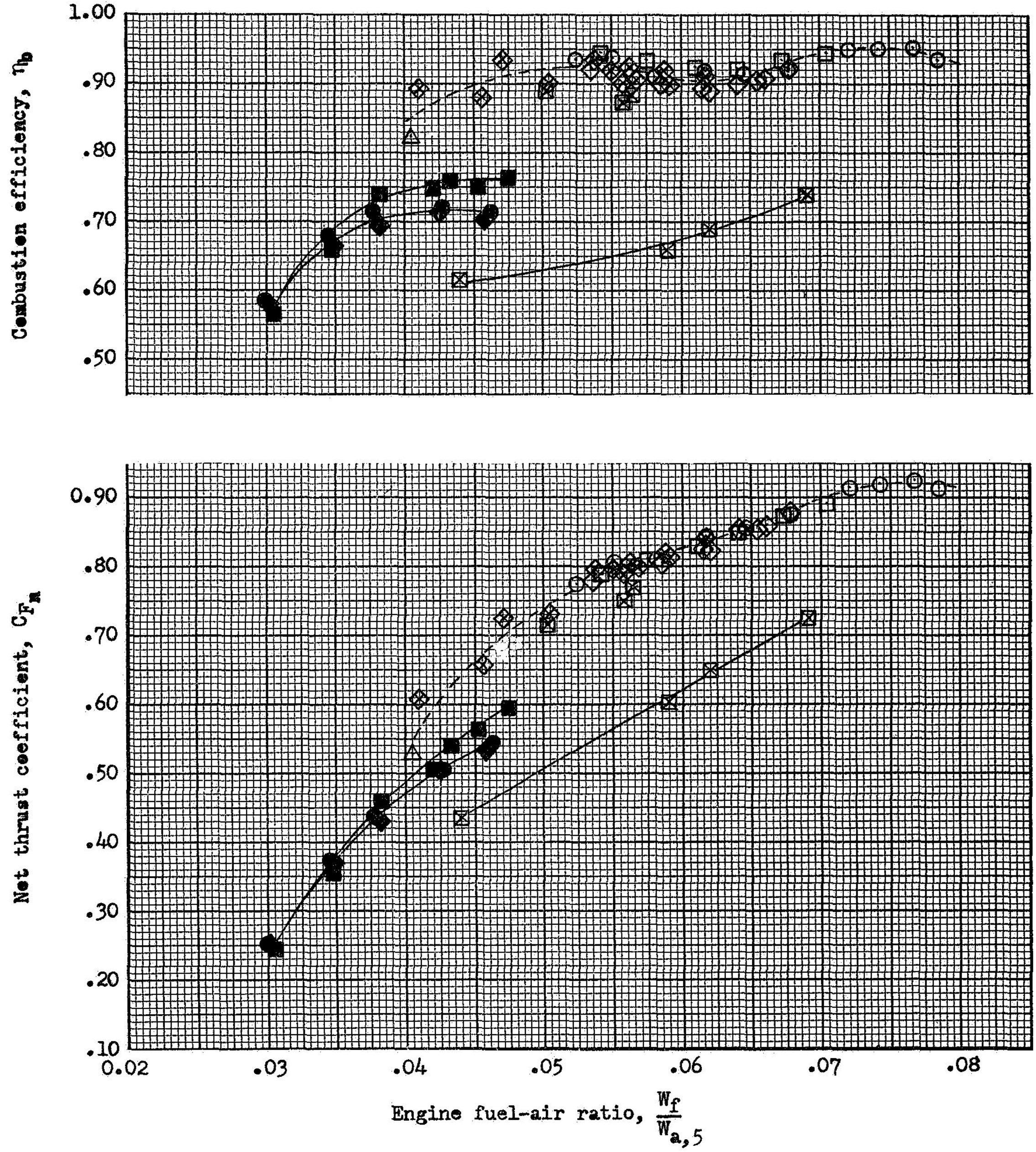

Figure 10. - Concluded. Engine performance. Altitude, 50,000 feet; inlet temperature, 790 °R (MCD).

3635

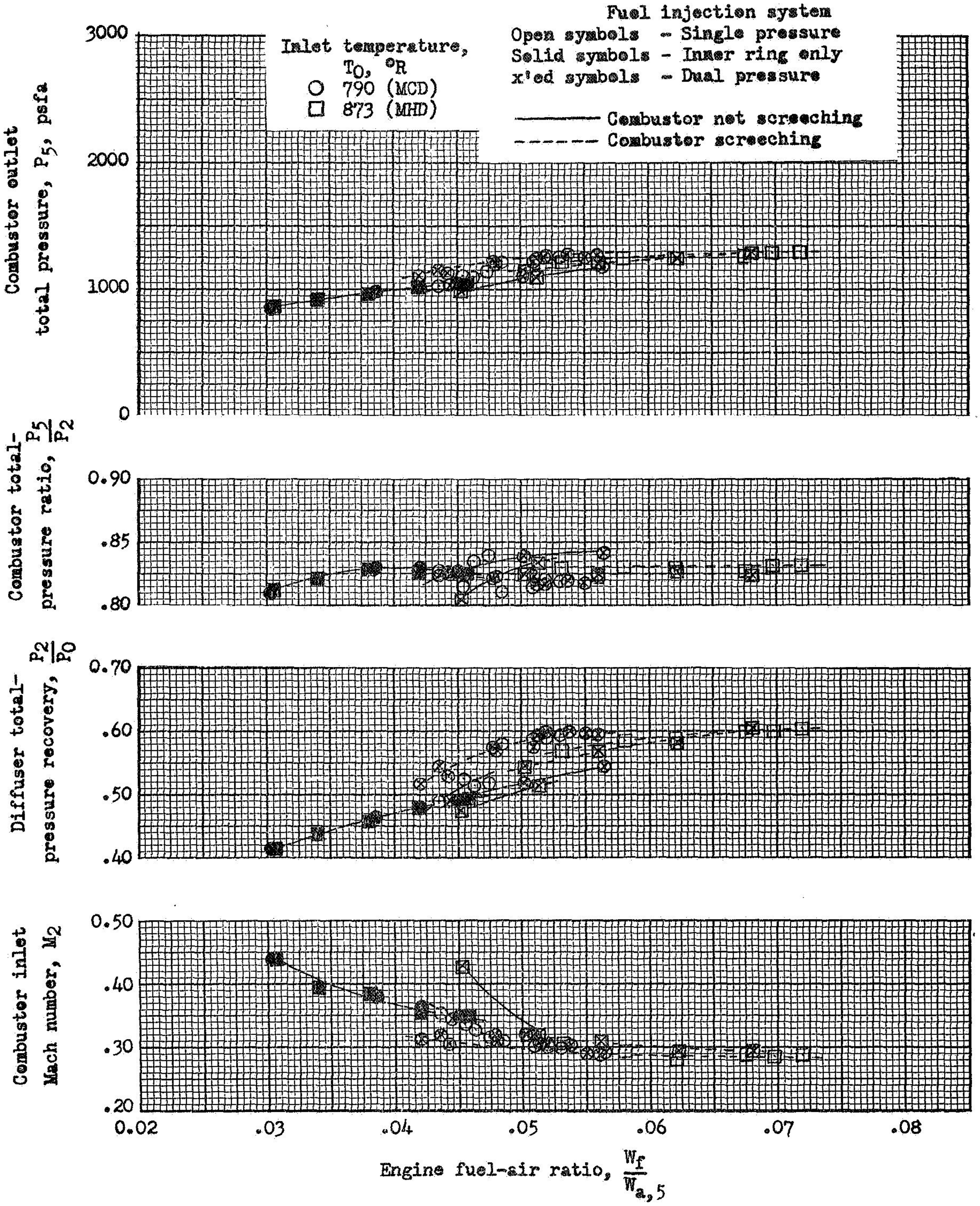

Figure 11. - Effect of inlet temperature on engine performance. Altitude, 60,000 feet; angle of attack, +4°.

DECLASSIFIED

3635

CX-6

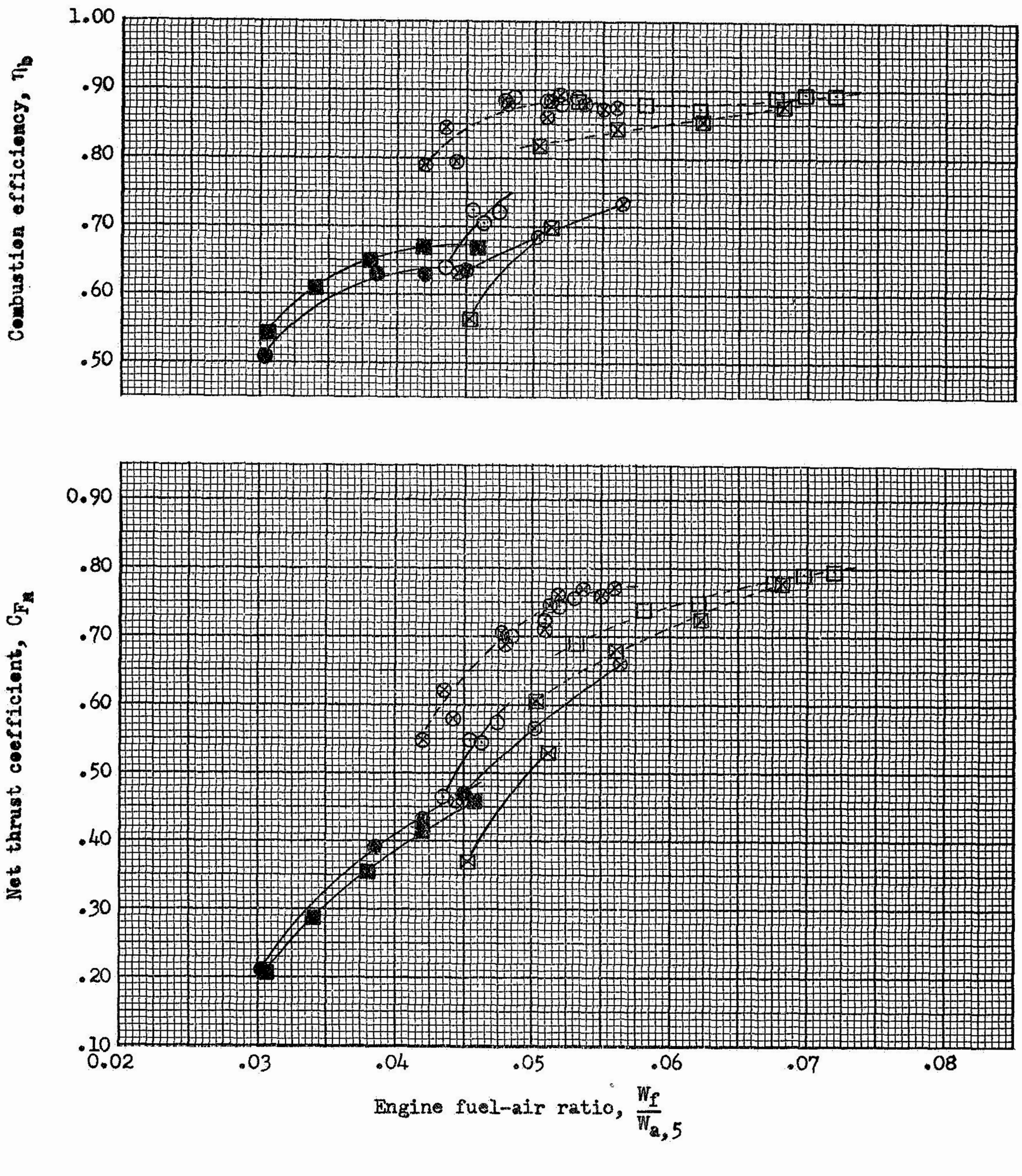

Figure 11. - Concluded. Effect of inlet temperature on engine performance. Altitude, 60,000 feet; angle of attack, +4°.

[redacted]

3635

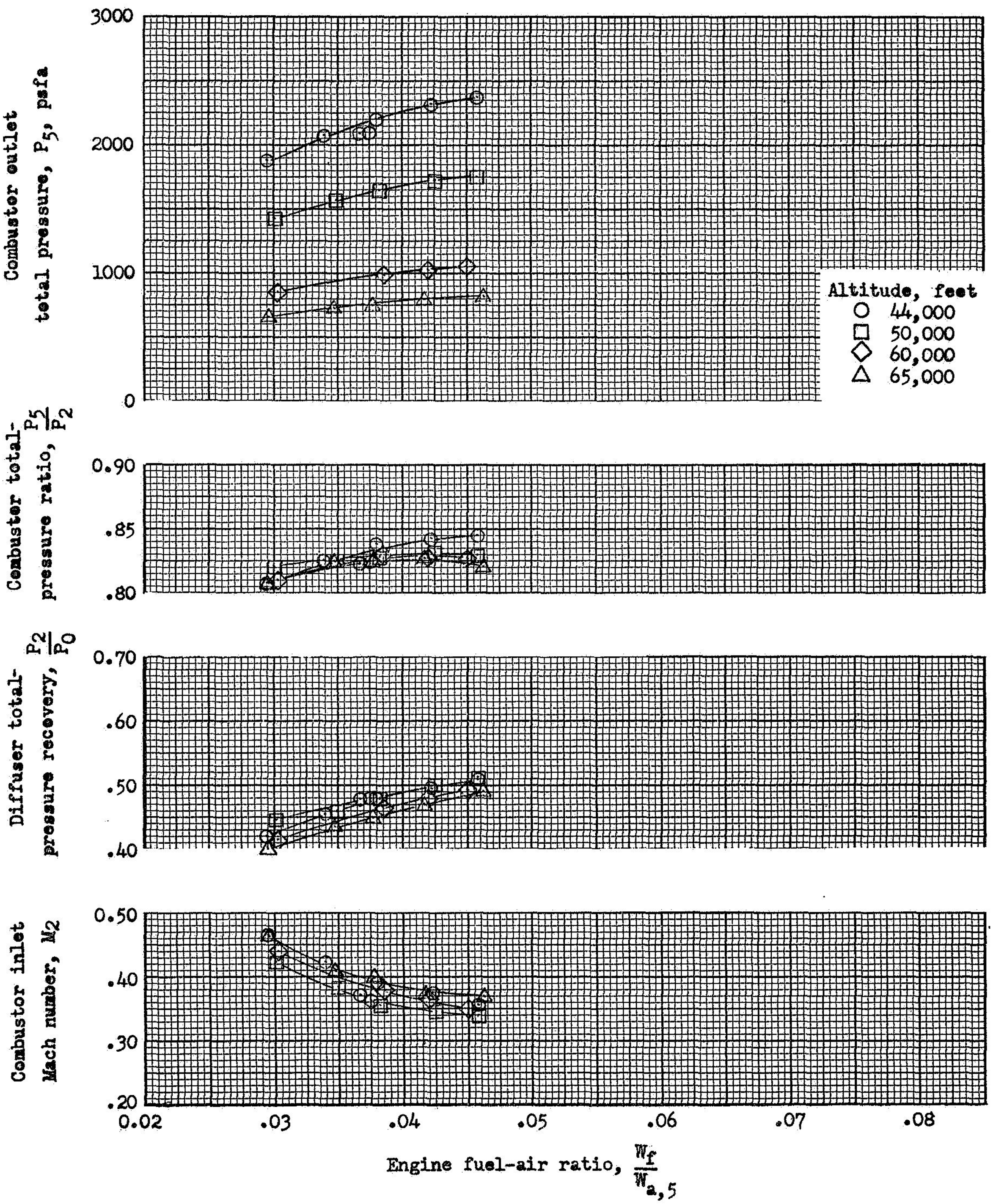

(a) Inner-ring-only fuel injection.

Figure 12. - Effect of altitude on engine performance. Miami cold day inlet temperature. Angle of attack, +4°.

3635

CX-6 back

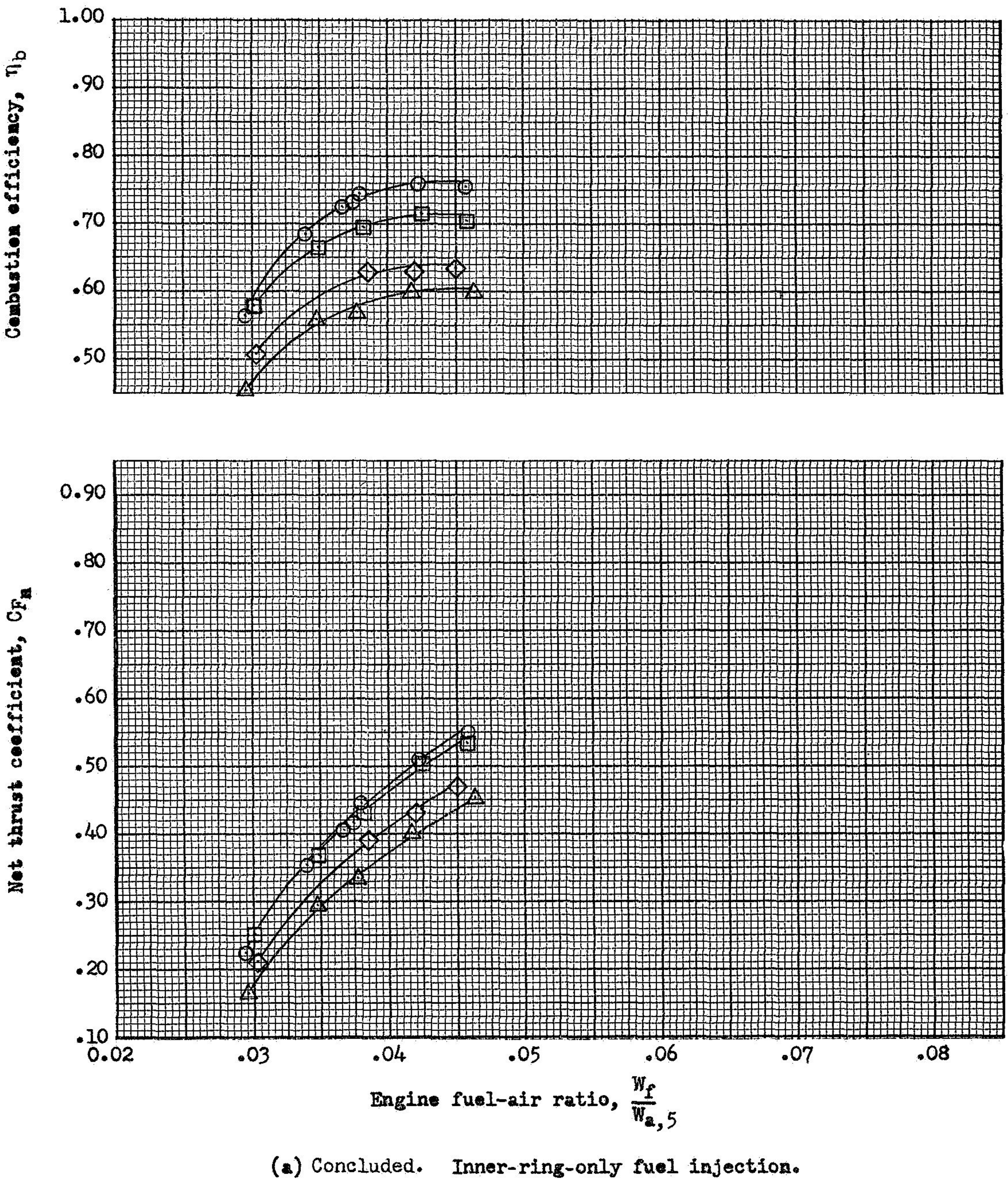

(a) Concluded. Inner-ring-only fuel injection.

Figure 12. - Continued. Effect of altitude on engine performance. Miami cold day inlet temperature. Angle of attack, +4°.

3635

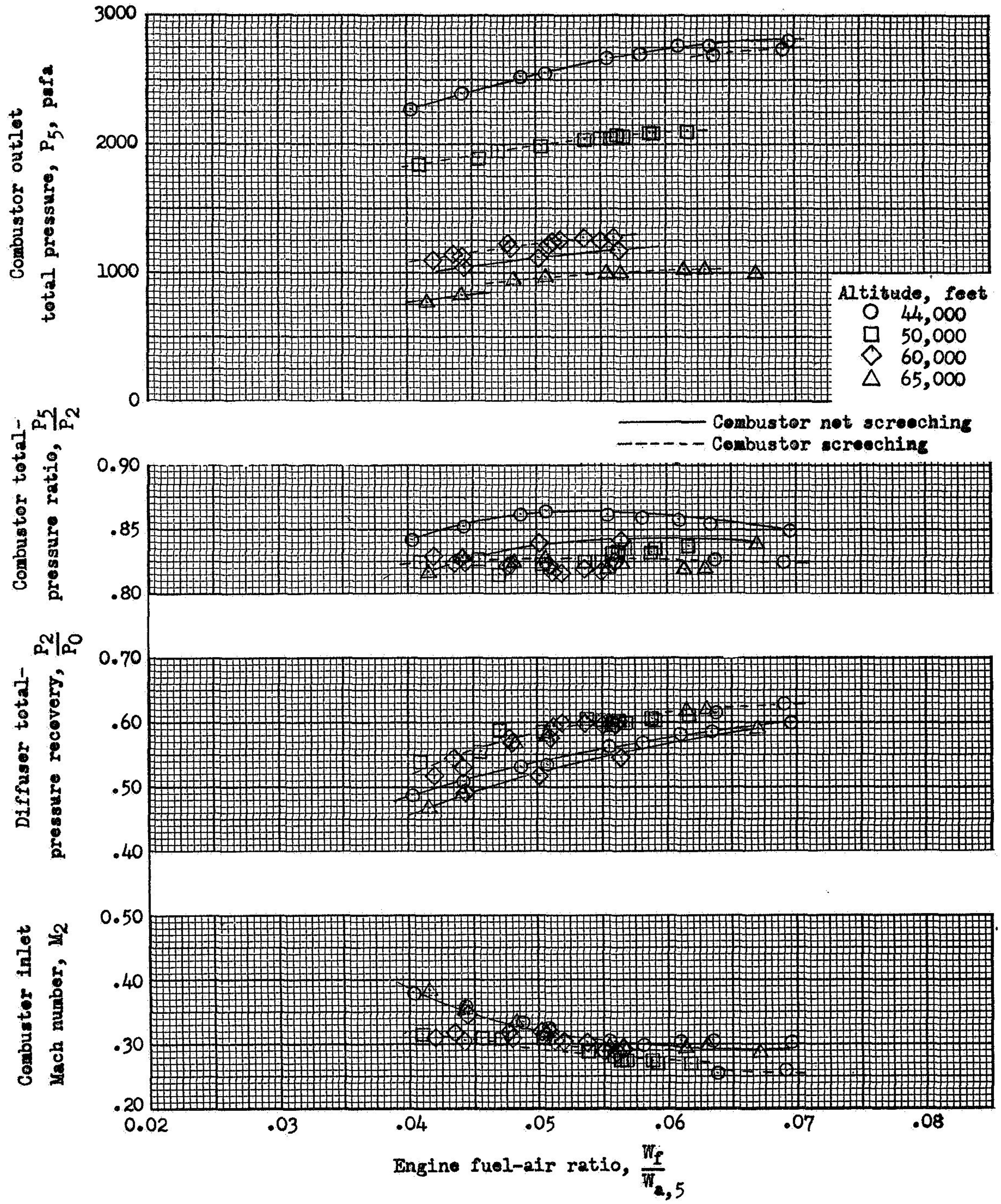

(b) Dual-pressure fuel injection.

Figure 12. - Continued. Effect of altitude on engine performance. Miami cold day inlet temperature. Angle of attack, +4°.

[redacted]

DECLASSIFIED

3635

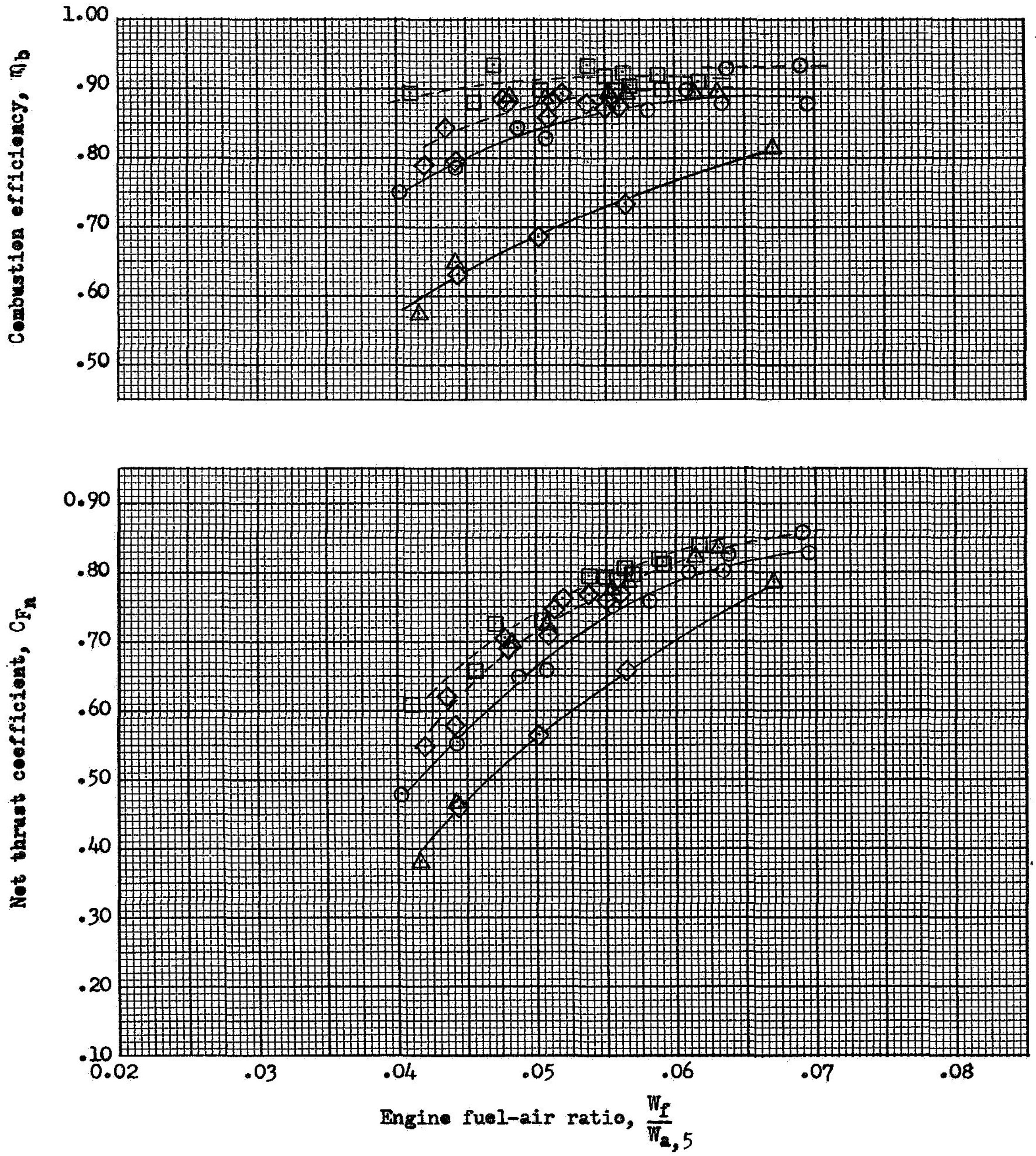

(b) Concluded. Dual-pressure fuel injection.

Figure 12. - Continued. Effect of altitude on engine performance. Miami cold day inlet temperature. Angle of attack, +4°.

3635

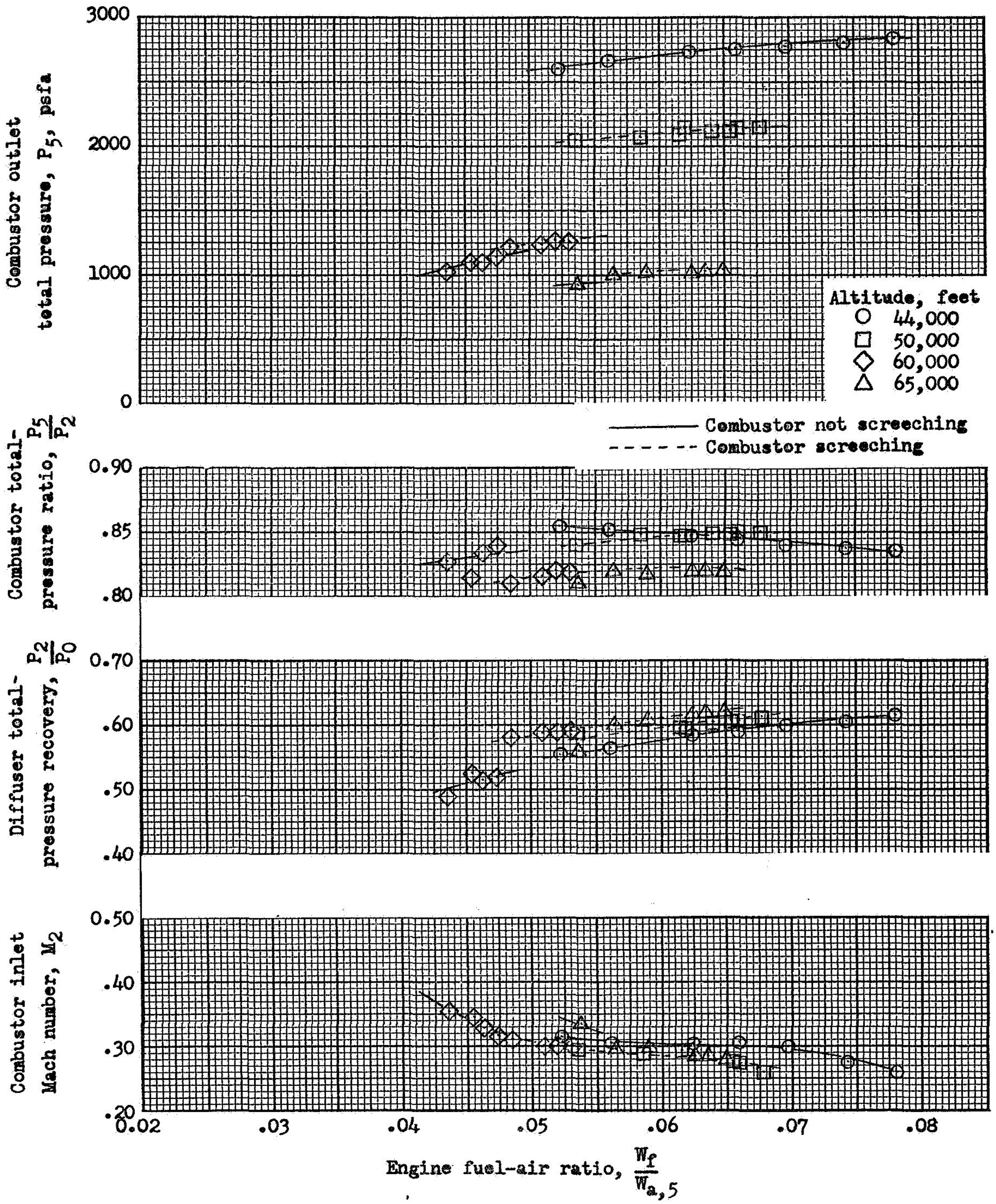

(c) Single-pressure fuel injection.

Figure 12. - Continued. Effect of altitude on engine performance. Miami cold day inlet temperature. Angle of attack, +4°.

[redacted]

DECLASSIFIED

3635

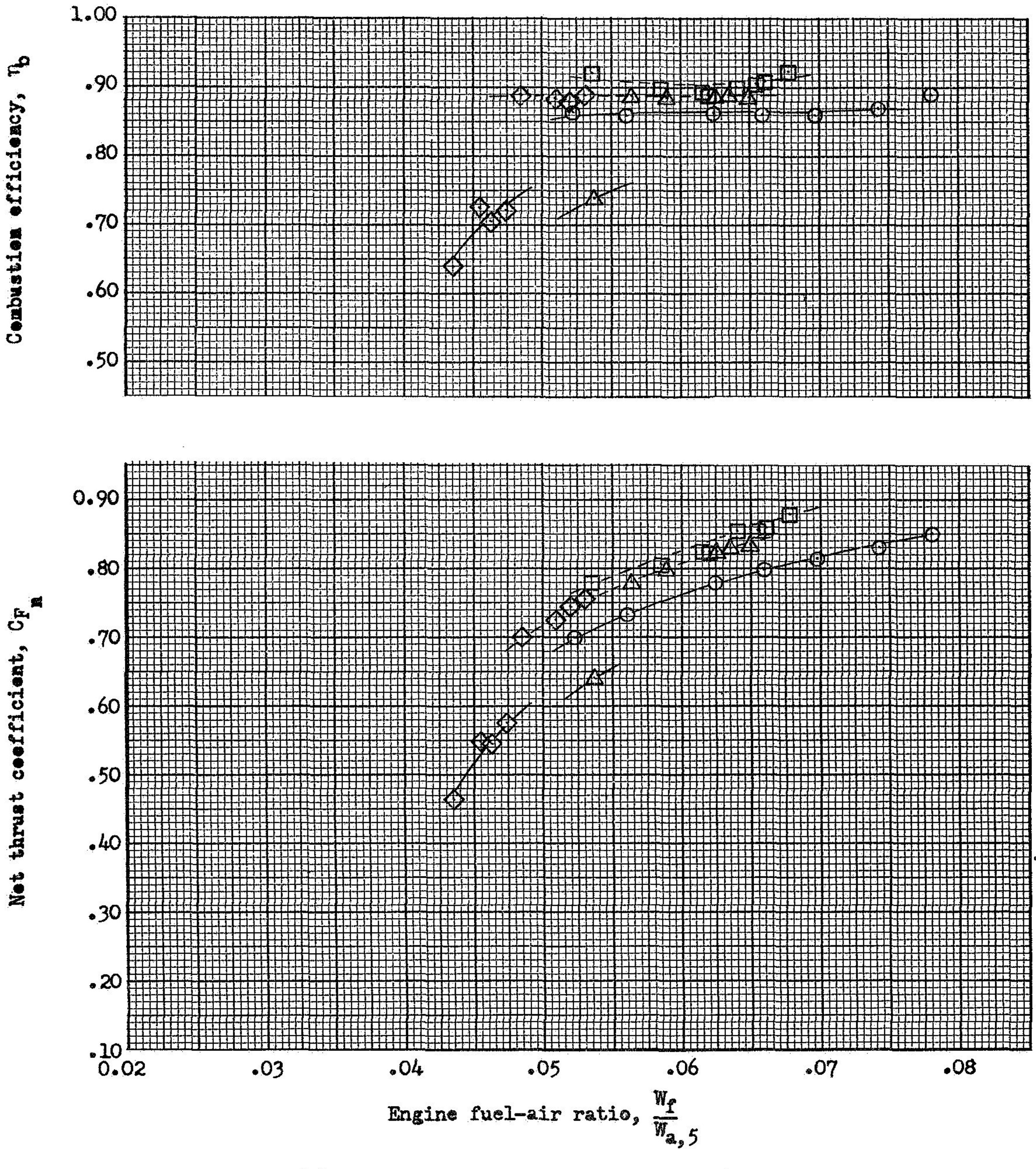

(c) Concluded. Single pressure fuel injection.

Figure 12. - Concluded. Effect of altitude on engine performance. Miami cold day inlet temperature. Angle of attack, +4°.

[redacted]

3635

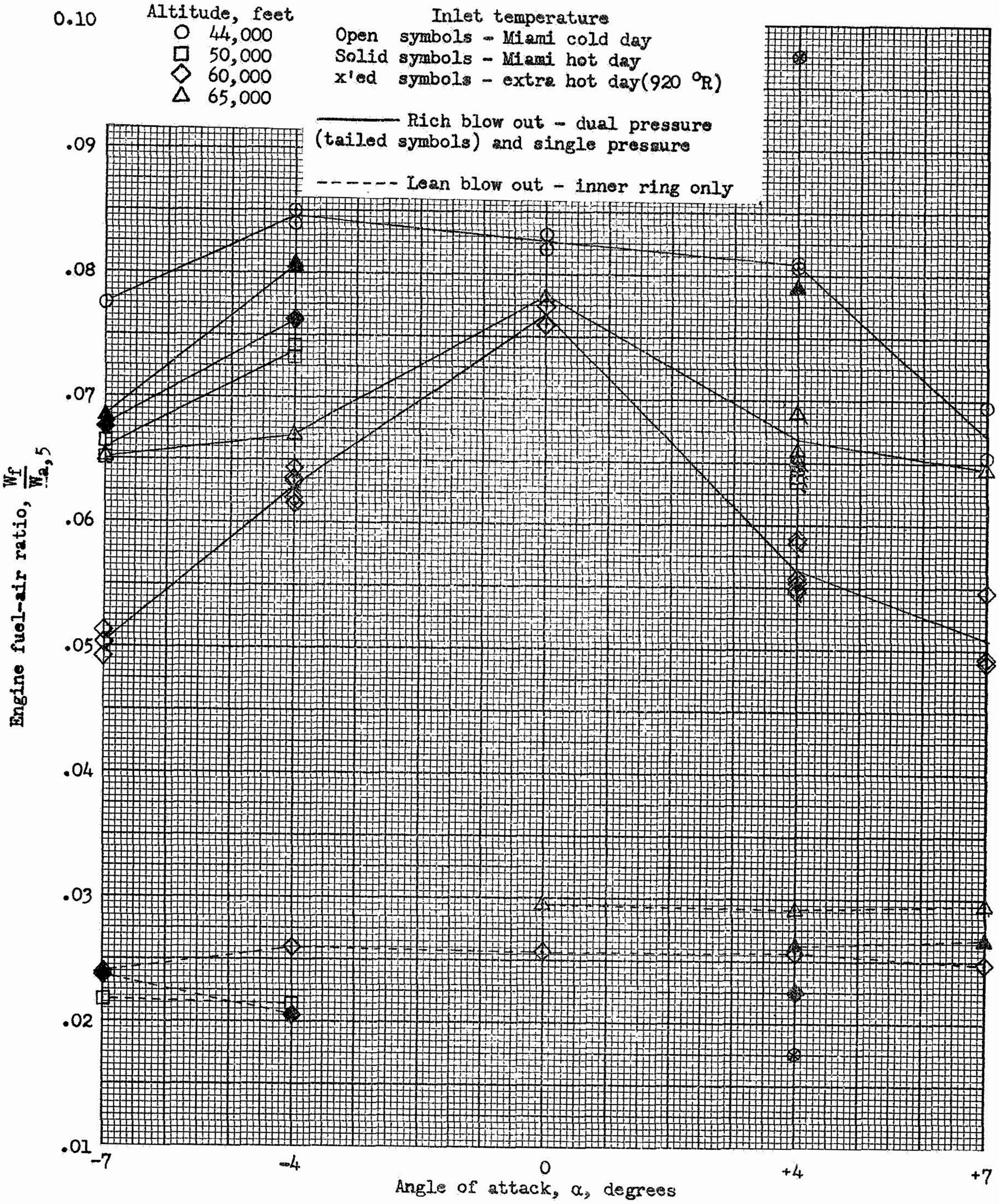

Figure 13. - Combustor blow-out limits.

DECLASSIFIED

3635

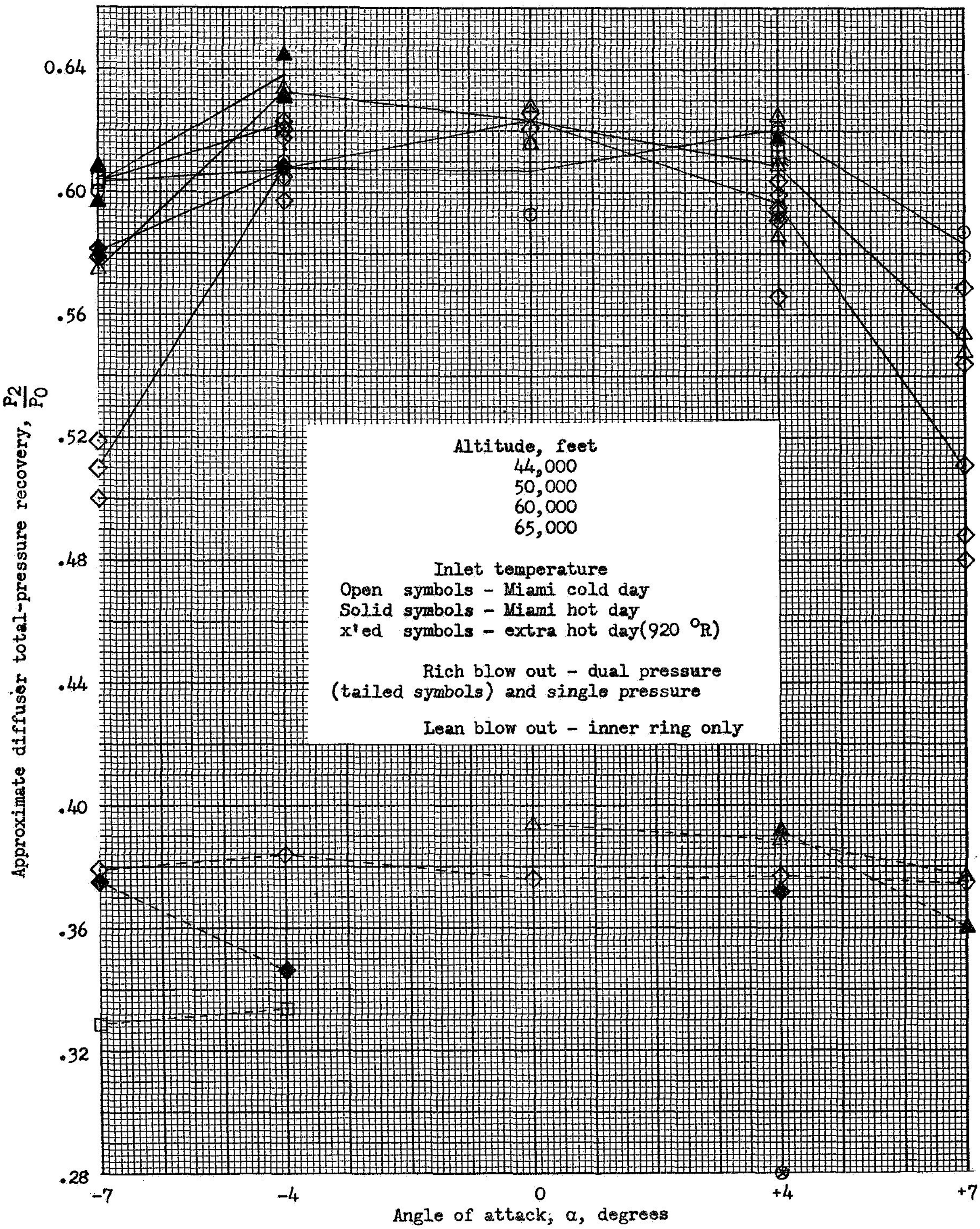

Figure 14. - Approximate diffuser total-pressure recovery at combustor blow-out.

[redacted]